AN ABSTRACT OF THE THESIS OF

FRANK BARRY MESEROLE for the degree Doctor of Philosophy
(Name of student) (Degree)

in Chemistry presented on August 6, 1974
(Major department) (Date)

Title: SPECTRAL INVESTIGATION OF THE MOLECULAR VIBRATION REGION OF SINGLE CRYSTALLINE POTASSIUM SULFATE

Redacted for privacy

Abstract approved: J. C. Decius

A spectral investigation of the molecular vibration region of the potassium sulfate crystal system was undertaken. This study was initiated to establish the feasibility of using this crystal as a host matrix for ammonium sulfate. Since these two systems are isomorphic and have unit cells of nearly equal volume the ammonium ion can be studied in a surrounding similar to that of the ammonium sulfate crystal with a variable degree of inter-ion coupling by doping the potassium sulfate crystal with different amounts of ammonium sulfate.

The potassium sulfate vibration region was characterized by infrared transmission and reflection measurements plus laser Raman scattering. A technique incorporating a reflection goniometer was

used to identify the habit of laboratory grown potassium sulfate crystals and to guide the preparation of faces perpendicular to each of the three principle axis. Spectra invoking polarized radiation were subsequently obtained from these faces and band assignments made on the basis of a correlation diagram.

Preliminary transmission investigations of ammonium doped potassium sulfate gave excellent results establishing the feasibility of this approach.

Spectral Investigation of the Molecular Vibration Region of Single Crystalline Potassium Sulfate

by

Frank Barry Meserole

A THESIS

submitted to

Oregon State University

in partial fulfillment of
the requirements for the
degree of

Doctor of Philosophy

June 1975

APPROVED:

Redacted for privacy

Professor of Chemistry in charge of major

Redacted for privacy

Chairman of Department of Chemistry

Redacted for privacy

Dean of Graduate School

Date thesis is presented August 6, 1974

Typed by ibid. inc. for Frank Barry Meserole

ACKNOWLEDGEMENTS

I would like to express my sincere appreciation and gratitude to Dr. J. C. Decius for his suggestions and guidance during this work and especially for his patience.

Deepest thanks also go to my wife Sue for her support and encouragement and to Marta Jaramillo for her understanding.

TABLE OF CONTENTS

TABLE OF CONTENTS (continued)

LIST OF TABLES

LIST OF FIGURES

LIST OF FIGURES (continued)

LIST OF FIGURES (continued)

LIST OF FIGURES (continued)

SPECTRAL INVESTIGATION OF THE MOLECULAR VIBRATION REGION OF SINGLE CRYSTALLINE POTASSIUM SULFATE

I. INTRODUCTION

The crystallographic structures of solid K_2SO_4 and $(NH_4)_2SO_4$, stable at room temperature, are isomorphous and can form solid solutions with each other. This presents the opportunity to isolate the ammonium ion at low concentrations in a lattice very similar to that of pure $(NH_4)_2SO_4$ by doping K_2SO_4 crystals with NH_4^+. At these low concentrations the intermolecular coupling between ammonium ions is greatly diminished as compared to the pure $(NH_4)_2SO_4$. Vibrational spectroscopy can therefore be used to determine the intermolecular potential function in $(NH_4)_2SO_4$ crystals once the spectra of pure K_2SO_4, pure $(NH_4)_2SO_4$ and dilute NH_4^+ in K_2SO_4 have been observed and analyzed.

The experimental results to be presented and discussed will include the following:

polarized infrared transmission spectra of oriented, thin crystalline sections of pure K_2SO_4.

polarized infrared reflection spectra of oriented K_2SO_4 crystals and near-normal and non-normal angles of incidence.

polarized laser-Raman spectra of oriented K_2SO_4 crystals.

non-polarized infrared transmission spectra of thin crystalline sections of pure $(NH_4)_2SO_4$.

polarized infrared transmission spectra of oriented, thin crystalline sections of NH_4^+ doped K_2SO_4.

The polarized spectra were accomplished by orienting the prepared faces of the crystals such that the selected electric vector of the

incident radiation was parallel to a known crystallographic axis.

Attempts to obtain infrared transmission spectra of pure, single crystals suffer from the difficult problem of obtaining sufficiently thin crystalline sections. According to the transmission equation for absorbing media, worked out by Born and Huang (5), pure absorption is never observed until the product of the sample thickness (d) times the absorption coefficient (k) is small compared with the radiation wavelength (λ). When this condition is not satisfied, reflection losses give broad absorption-like bands in the region between ν_T and ν_L for a given mode. The separation of ν_T and ν_L is determined by the dipole derivative of the vibrational mode as is the absorption coefficient. Modes having large dipole derivatives give broad absorptions (100-300 cm^{-1}) even at relatively thin cross-sections. Based upon the author's experience with the K_2SO_4 and $(NH_4)_2SO_4$ systems, the pure absorption spectra in the region of fundamental $SO_4^{=}$ vibrations, ν_3 and ν_4, would not be observed until the crystal thickness was less than 1 μ. Since thin films of single crystals of this thickness appear to be unattainable at the present time, other sampling techniques were investigated.

Both K_2SO_4 and $(NH_4)_2SO_4$ spectra have been obtained using mulling techniques. For non-cubic systems, however, this technique results in a superposition of the components of the various symmetry species, thus making a detailed assignment impossible even when the components are resolved.

Doping techniques are possible if a suitable host can be found. The ammonium ion can be studied in the K_2SO_4 system, but the degree

of application of the data to the pure $(NH_4)_2SO_4$ system depends very highly on the nature of the host. As mentioned previously K_2SO_4 exhibits the same lattice structure as $(NH_4)_2SO_4$ and has unit cell dimensions very nearly the same, the NH_4^+ can therefore fit into the K_2SO_4 lattice with very little distortion due to steric effects. The hydrogen bonding with the sulfate oxygens will be nearly the same in the host as in the pure $(NH_4)_2SO_4$ and the site symmetry of NH_4^+ will be the same. As the concentration of the NH_4^+ in the host approaches infinite dilution, the intermolecular interactions between ammonium ions will vanish. Extrapolation of the frequencies obtained for various low concentrations of NH_4^+ to zero concentration will give the characteristic vibrational frequencies approximating the "decoupled" system.

As a prerequisite to using K_2SO_4 as a host crystal for NH_4^+, the K_2SO_4 system itself must be understood and of course any absorptions in or near the regions of absorption of NH_4^+ must be known and well characterized. It is then the intended purpose of this work to provide a comprehensive study of K_2SO_4 as well as some preliminary work involving doped NH_4^+. In many instances, however, due to the complexity of the system the experimental results are merely reported, leaving an interpretation to future investigators.

As mentioned previously three sources of data have been utilized in an effort to characterize spectroscopically the single crystalline state of K_2SO_4 according to the polarizability of the components of the vibrational absorptions along the three principle crystallographic axes. Polarized laser Raman, polarized infrared

transmission and polarized infrared reflection spectroscopical techniques were used as both supplementary, in the case of infrared vs. Raman, and complementary, in the case of infrared transmission vs. reflection, means of identifying as many as possible of the symmetry predicted components arising from fundamental vibrational transitions. Also included are the experimental results involving non-normal incidence reflection measurements on K_2SO_4 crystals. D. W. Berreman (4) has shown that the longitudinal optic frequencies in cubic crystal films can be measured by infrared absorption when the incident radiation is not normal to the crystal surface.

II. PREVIOUS INVESTIGATIONS ON THE K_2SO_4 AND $(NH_4)_2SO_4$ CRYSTAL SYSTEMS

Earlier spectrographic work on the K_2SO_4 and $(NH_4)_2SO_4$ crystal include x-ray characterization, Raman and infrared analyses. The x-ray results led to a crystallographic description of the crystals which included unit cell dimensions and identification of the crystal system. The Raman and infrared studies were quite general and gave very little polarization information.

A. Crystal Parameters as Determined by X-Ray Scattering

The room temperature phases of K_2SO_4 and $(NH_4)_2SO_4$ are found to form orthorhombic crystals with the following unit cell dimensions (18):

K_2SO_4	$(NH_4)_2SO_4$
a = 5.731Å	a = 5.951Å
b = 10.008Å	b = 10.560Å
c = 7.424Å	C = 7.729Å

The crystals belong to the space group D_{2h}^{16} with four molecules per unit cell. The sulfate ions are situated on sites of C_s symmetry with the plane of symmetry corresponding to the yz crystallographic plane.

Table 1 shows the linear coordinates of the atoms of K_2SO_4 in a unit cell and Figures 1, 2 and 3 give the three projections

Table 1. Coordinates of the atoms of the four molecules of K_2SO_4 in a unit cell given in angstroms along the three orthogonal axes

Molecule	Atom	a (Å)	b (Å)	c (Å)
A	S	4.30	5.84	5.54
	O	"	"	7.06
	O	"	4.43	5.04
	O	5.52	6.54	"
	O	3.08	"	"
	K	4.30	5.84	2.38
	K	"	6.84	7.42
B	S	4.30	9.18	1.83
	O	"	"	3.35
	O	"	0.58	1.33
	O	5.52	8.48	"
	O	3.08	"	"
	K	4.30	9.18	6.09
	K	"	8.18	3.71
C	S	1.43	0.83	5.59
	O	"	"	4.07
	O	"	-0.58	6.09
	O	0.21	1.53	"
	O	2.65	"	"
	K	1.43	0.83	1.33
	K	"	1.83	3.71
D	S	1.43	4.17	1.88
	O	"	"	0.36
	O	"	5.58	2.38
	O	0.21	3.47	"
	O	2.65	"	"
	K	1.43	4.17	5.04
	K	"	3.17	0.00

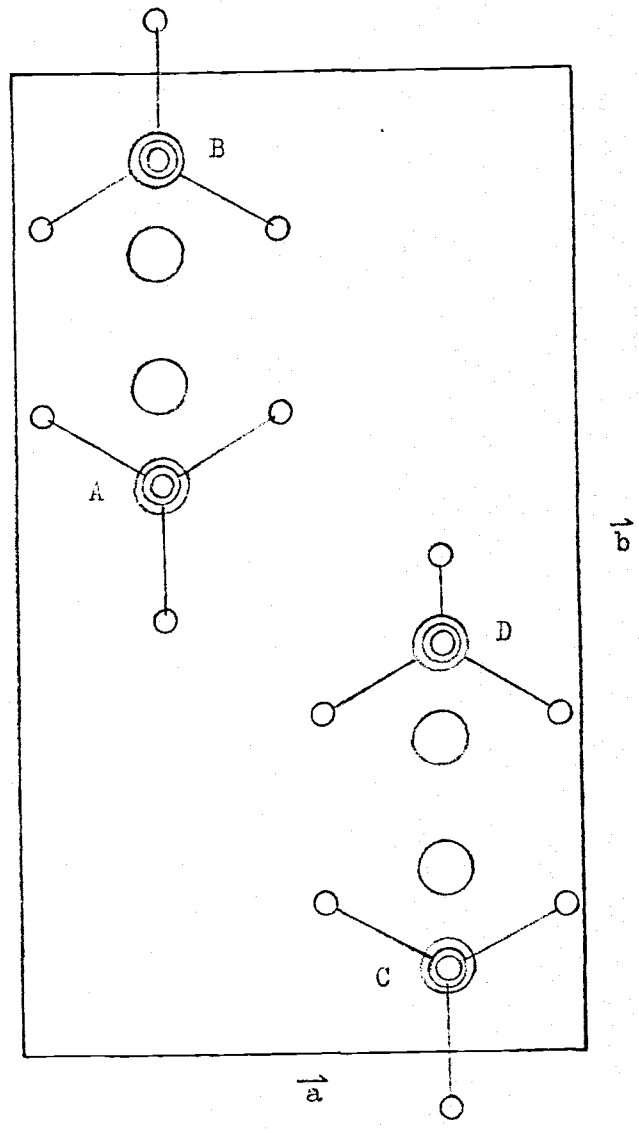

Figure 1. Projection of the four K_2SO_4 molecules per unit cell upon the ab plane. The largest circles represent potassium ions with the smallest circles representing oxygen atoms with bonds to the sulfur atoms

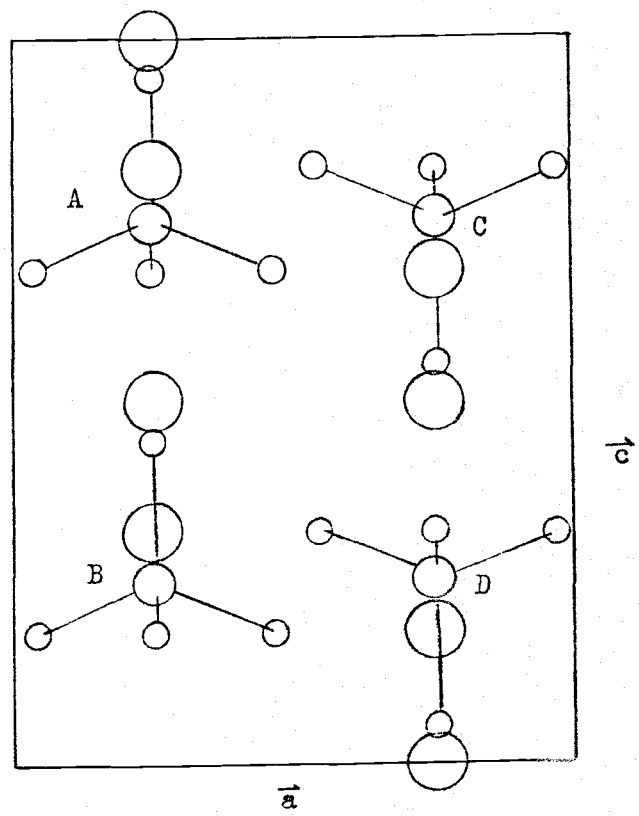

Figure 2. Projection of the four K_2SO_4 molecules per unit cell upon the ac plane. The largest circles represent potassium ions with the smallest circles representing oxygen atoms with bonds to the sulfur atoms

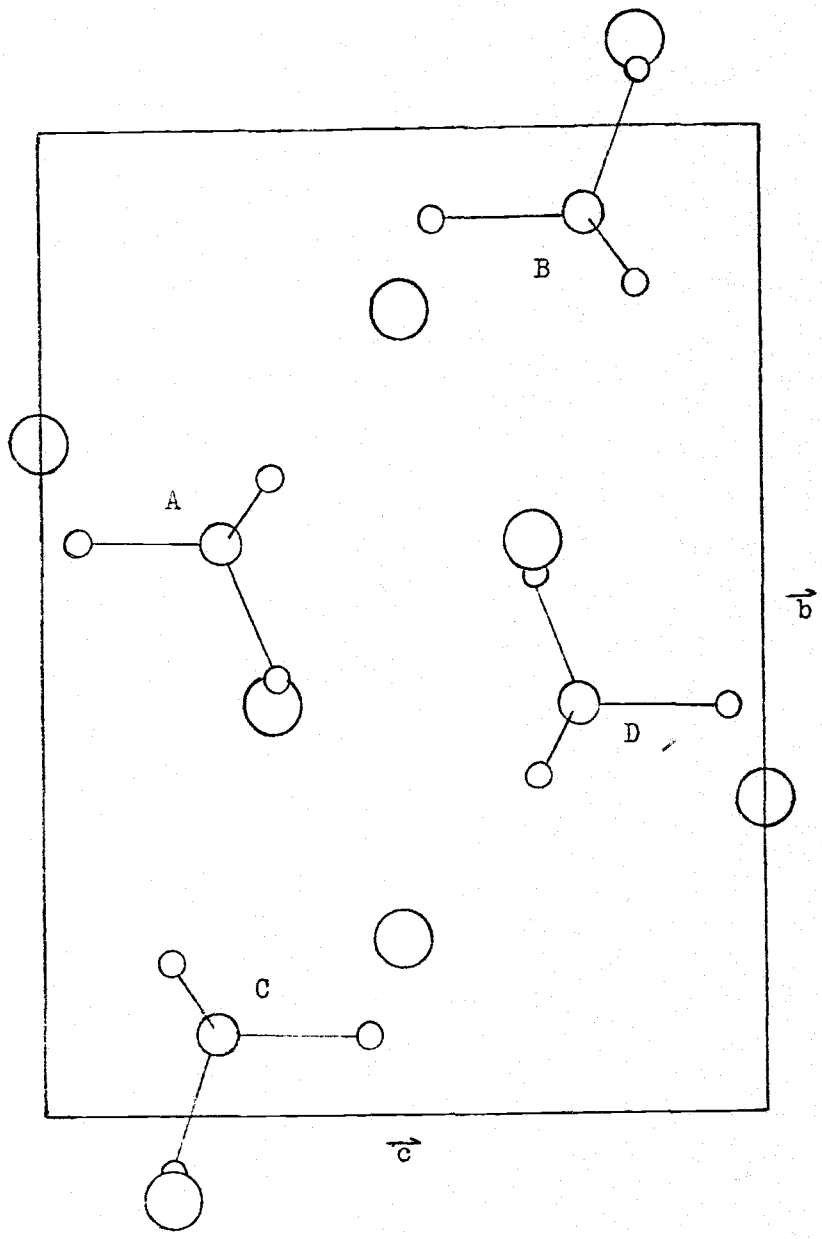

Figure 3. Projection of the four K_2SO_4 molecules per unit cell upon the bc plane. The largest circles represent potassium ions with the smallest circles representing oxygen atoms with bonds to the sulfur atoms

of the unit cell along the crystallographic axes. These projections should give some insight into the interpretation of the following spectra.

B. Previous Raman Spectra of K_2SO_4

V. Ananthanarayanan (1) reported the results of Raman spectra of K_2SO_4. Single crystals were used, but the spectra were not taken along the principal axes. The incident radiation (λ = 2536.5Å) was normal to the 110 face and the scattered radiation was taken parallel to the 110 face and nearly perpendicular to the 001 face. This experimental arrangement gave all of the allowed Raman absorptions, but no information as to relative intensities and symmetry species could be obtained. The use of a He-Ne laser as a source combined with the use of oriented samples and polarized light have given more information about the nature of the vibrational states. These results will be presented in a later section along with a comparison of Ananthanarayanan's work.

C. Previous I.R. Transmission Data on K_2SO_4

Schroeder, Kippincott, and Weir (19) reported in 1965 on K_2SO_4 transmission spectra of thin sections of 25-250μ thick. Though single crystals were used the spectra shown appear to be the results of unpolarized absorption on thin sections prepared coplanar with the largest naturally occurring face, namely 021.

They had the same sampling problems as were encountered in this work: sample thicknesses too great for resolution of the ν_3 and ν_4 regions. From the combination bands they were able to predict five components of ν_3 and three components of ν_4. There was, however, no attempt to describe the polarizations of the fundamental components of any of the regions and, consequently no assignments of the observed or deduced frequencies to unit cell symmetry species could be made. Their work did include much low temperature study and the relative intensities of the components resolved under these conditions allows a somewhat better check of predicted combination intensity rules than the room temperature spectra.

III. SAMPLE PREPARATION

Various sized crystals of K_2SO_4 and $(NH_4)_2SO_4$ were grown from saturated aqueous solutions according to the physical requirements of the spectroscopic measurements. In order to produce faces parallel to the crystallographic axes the crystal habit was identified and artificial faces prepared at specified angles to the natural faces.

A. Method of Crystal Growth

Baker's "Reagent" grade K_2SO_4 and $(NH_4)_2SO_4$ were used to produce the saturated solutions from which the crystals were grown. Small crystals were obtained by allowing a saturated aqueous solution to slowly evaporate at room temperature after the method described by Buckley (7). The small crystals grown as a result of spontaneous nucleation were harvested after a day or two. The crystals were removed from the mother liquor and quickly dried by sponging with absorbant tissues. Using a small magnifying lens a few crystals that appeared to be singular and of regular shape were selected to be used as seed crystals for growing larger crystals.

The seed crystals were connected to a section of monofilament thread by means of a small, knotted loop and suspended in a saturated solution by connecting the other end of the thread to a piece of bent wire referred to as a cobra. The upper end of the wire was kept below the surface of the solution to reduce the possibility

of extraneous crystals from growing on the thread, dislodging and subsequently contaminating the surfaces of the large crystal. The crystals were allowed to grow by slow evaporation of the water from the saturated solution for a period of one to six weeks depending on the type of crystal and the desired size. At the appropriate times the crystals were removed from the liquor and quickly dried, again using an absorbant material. Crystals produced by this method were generally well faceted and optically transparent in the visible region.

B. Identification of the Crystal Habit

Once a crystal of the desired size and appearance was grown, the next step involved the identification of the morphological habit that the crystal had grown in. This was accomplished with the aid of a reflecting goniometer. The goniometer consists of a calibrated disc mounted on a stand which also supports a light source and an eyepiece as shown in Figure 4. A crystal is mounted at the center of the disc and the disc is rotated until a crystal face is perpendicular to the bisector of the angle between the light and the eyepiece. At this point a strong reflection is observed at the eyepiece. The position of the disc at maximum reflection from a given face is recorded and the crystal is rotated until a reflection is observed due to the face adjacent the original face. Again the position of the disc is recorded and now the angle through which

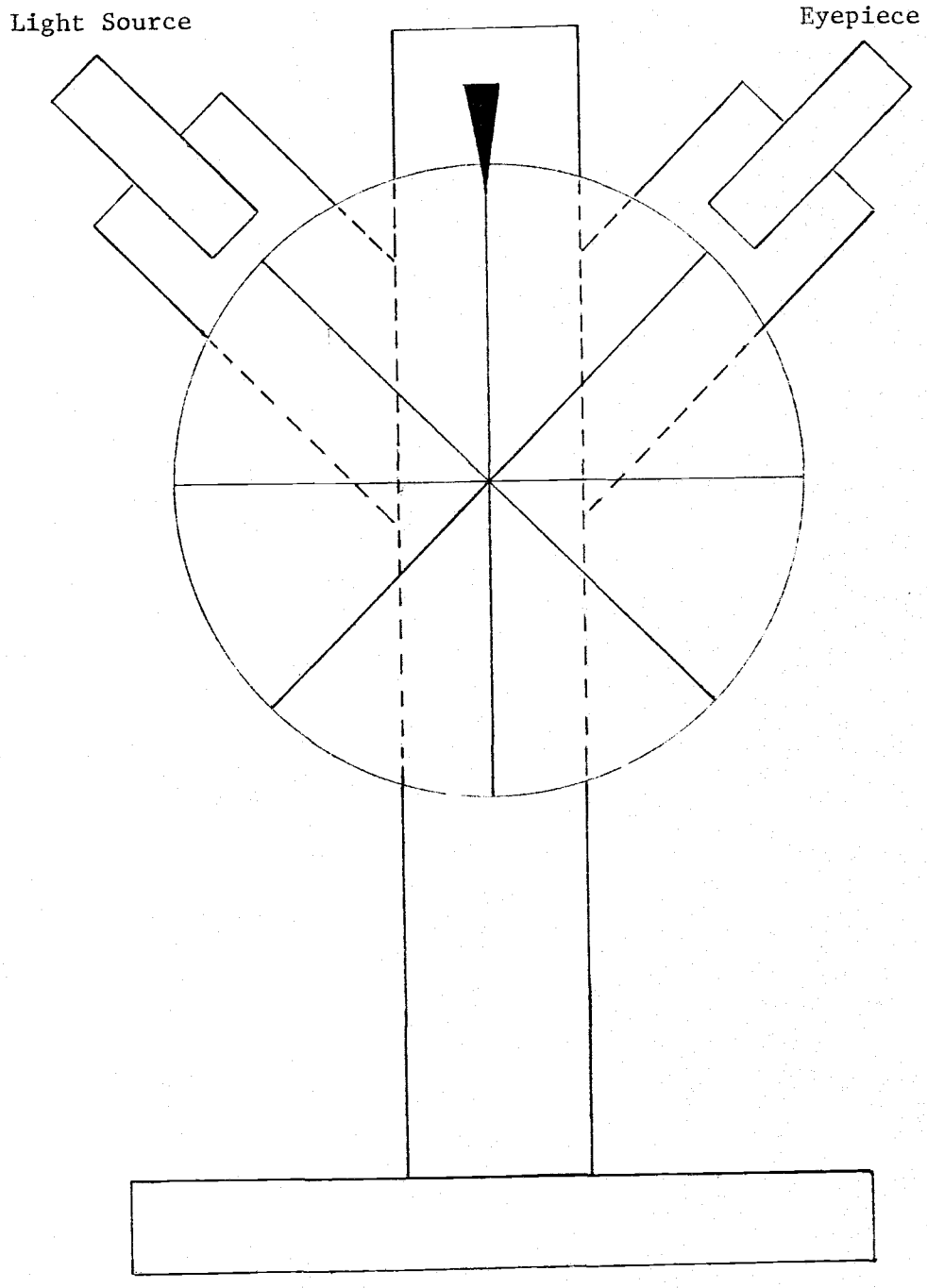

Figure 4. Reflection Goniometer

the crystal was rotated to bring two adjacent faces into the same plane is known. The angle between the two faces is then simply 180 minus the measured angle. The procedure is repeated until the angles between all of the naturally occurring faces have been determined.

It has been observed that the naturally occurring faces of a crystal can be described as being planes with Miller indices of small whole numbers, as 110, 021, 101, etc. A table is prepared listing the values of the angles between all possible faces having low Miller indices. These angles can be calculated for a crystal for which the unit cell dimensions and the crystal system are know. By comparing the values of the measured angles to the values listed in the table and maintaining a consistent sequence, the morphology of the crystal can be determined.

Tables 2, 3 and 4 give a listing of the calculated angles for several possible faces of K_2SO_4 and $(NH_4)_2SO_4$ and a listing of the general formulas for calculating these angles for any orthorhombic system in terms of the unit cell dimensions. The angles that were calculated are limited to faces parallel to specific axes.

The most common habit of K_2SO_4 encountered by the evaporation methods used was one in which the long morphological axis coincided with the shortest unit cell dimension, the a axis. The largest naturally occurring faces were the 021 type with somewhat smaller faces of the 011 type also present. Table 5 shows a cross-section

Table 2. Calculated Angles Between Faces Parallel to A Axis

Angle	General Term	K_2SO_4	$(NH_4)_2SO_4$
∠010,011	Arctan c/b + 90°	126°32'	126°10'
∠010,021	Arctan 2c/b + 90°	145°59'	145°38'
∠010,012	Arctan c/2b + 90°	111°43'	111°28'
∠001,011	Arctan b/c + 90°	143°27'	144° 2'
∠001,021	Arctan b/2c + 90°	123°49'	124°34'
∠001,012	Arctan 2b/c + 90°	159°40'	160° 3'
∠011,0$\bar{1}$1	2Arctan b/c	106°54'	108° 4'
∠011,01$\bar{1}$	2Arctan c/b	73° 4'	72°20'
∠011,0$\bar{1}$2	Arctan b/c + Arctan 2b/c	123° 7'	124° 5'
∠011,01$\bar{2}$	Arctan c/b + Arctan c/2b	58°15'	57°38'
∠011,012	Arctan b/c + Arctan c/2b + 90°	165°10'	165°30'
∠011,021	Arctan c/b + Arctan b/2c + 90°	160°31'	160°44'
∠011,0$\bar{2}$1	Arctan b/c + Arctan b/2c	87°26'	88°36'
∠011,02$\bar{1}$	Arctan c/b + Arctan 2c/b	92°32'	91°48'
∠021,02$\bar{1}$	2Arctan 2c/b	111°58'	111°16'
∠021,0$\bar{2}$1	2Arctan b/2c	67°58'	69° 8'
∠021,012	Arctan c/2b + Arctan b/2c + 90°	145°42'	146° 2'
∠021,0$\bar{1}$2	Arctan b/2c + Arctan 2b/c	103°39'	104°37'
∠021,01$\bar{2}$	Arctan 2c/b + Arctan c/2b	77°42'	77° 6'
∠012,0$\bar{1}$2	2Arctan 2b/c	139°20'	140° 6'
∠012,01$\bar{2}$	2Arctan c/2b	43°26'	42°56'

Table 3. Calculated Angles Between Faces Paralled to B Axis

Angle	General Term	K_2SO_4	$(NH_4)_2SO_4$
$\angle 100,101$	Arctan c/a + 90°	142°20'	142°23'
$\angle 100,201$	Arctan 2c/a + 90°	158°53'	158°56'
$\angle 100,102$	Arctan c/2a + 90°	122°57'	122°59'
$\angle 001,101$	Arctan a/c + 90°	127°41'	127°37'
$\angle 001,201$	Arctan a/2c + 90°	111° 7'	111° 5'
$\angle 001,102$	Arctan 2a/c + 90°	147° 5'	147° 2'
$\angle 101,\bar{1}01$	2Arctan a/c	75°22'	75°14'
$\angle 101,10\bar{1}$	2Arctan c/a	104°40'	104°46'
$\angle 101,\bar{1}02$	Arctan a/c + Arctan 2a/c	94°46'	94°39'
$\angle 101,10\bar{2}$	Arctan c/a + Arctan c/2a	85°17'	85°22'
$\angle 101,102$	Arctan a/c + Arctan c/2a + 90°	160°38'	160°36'
$\angle 101,201$	Arctan c/a + Arctan a/2c + 90°	163°27'	163°27'
$\angle 101,\bar{2}01$	Arctan a/c + Arctan a/2c	58°48'	58°42'
$\angle 101,20\bar{1}$	Arctan c/a + Arctan 2c/a	121°13'	121°19'
$\angle 201,20\bar{1}$	2Arctan 2c/a	137°46'	137°52'
$\angle 201,\bar{2}01$	2Arctan a/2c	42°14'	42°10'
$\angle 201,102$	Arctan c/2a + Arctan a/2c + 90°	144° 4'	144° 4'
$\angle 201,\bar{1}02$	Arctan a/2c + Arctan 2a/c	78°12'	78° 7'
$\angle 201,10\bar{2}$	Arctan 2c/a + Arctan c/2a	101°50'	101°55'
$\angle 102,\bar{1}02$	2Arctan 2a/c	114°10'	114° 4'
$\angle 102,10\bar{2}$	2Arctan c/2a	65°54'	65°58'

Table 4. Calculated Angles Between Faces Paralled to C Axis

Angle	General Term	K_2SO_4	$(NH_4)_2SO_4$
∠100,110	Arctan b/a + 90°	150°13'	150°36'
∠100,210	Arctan 2/ba + 90°	164° 2'	164°18'
∠100,120	Arctan b/2a + 90°	131° 9'	131°36'
∠010,110	Arctan a/b + 90°	119°47'	119°24'
∠101,210	Arctan a/2b + 90°	104°58'	104°44'
∠010,120	Arctan 1a/b + 90°	138°52'	138°25'
∠110,$\bar{1}$10	2Arctan a/b	59°34'	58°48'
∠110,1$\bar{1}$0	2Arctan b/a	120°26'	121°12'
∠110,$\bar{1}$20	Arctan a/b + Arctan 2a/b	78°39'	77°49'
∠110,1$\bar{2}$0	Arctan b/a + Arctan b/2a	101°22'	102°12'
∠110,120	Arctan a/b + Arctan b/2a + 90°	160°56'	161°
∠110,210	Arctan b/a + Arctan a/2b + 90°	166°11'	166°20'
∠110,$\bar{2}$10	Arctan a/b + Arctan a/2b	45°45'	45° 8'
∠110,2$\bar{1}$0	Arctan b/a + Arctan 2b/a	134°15'	134°54'
∠210,2$\bar{1}$0	2Arctan 2b/a	148° 4'	148°36'
∠210,$\bar{2}$10	2Arctan a/2b	31°56'	31°28'
∠210,120	Arctan b/2a + Arctan a/2b + 90°	147° 7'	147°20'
∠210,$\bar{1}$20	Arctan a/2b + Arctan 2a/b	64°50'	56° 9'
∠201,1$\bar{2}$0	Arctan 2b/a + Arctan b/2a	115°11'	115°54'
∠120,$\bar{1}$20	2Arctan 2a/b	97°54'	96°50'
∠120,1$\bar{2}$0	2Arctan b/2a	82°18'	83°12'

Table 5. Assignment of the Faces of a Typical K_2SO_4 Crystal

Measured Values	Calculated Values Parallel to A Axis
$\angle 1,2 = 145°36'$	$\angle 010,021 = 145°59'$
$\angle 2,3 = 160°18'$	$\angle 021,011 = 160°31'$
$\angle 3,4 = 107°$	$\angle 011,0\bar{1}1 = 106°54'$
$\angle 4,5 = 160°36'$	$\angle 0\bar{1}1,0\bar{2}1 = 160°31'$
$\angle 5,6 = 111°42'$	$\angle 0\bar{2}1,0\bar{2}\bar{1} = 111°58'$
$\angle 6,7 = 68°28'$	$\angle 0\bar{2}\bar{1},02\bar{1} = 67°58'$
$\angle 7,1 = 146°30'$	$\angle 02\bar{1},010 = 145°59'$

ASSIGNED FACES

Face #1 = 010

#2 = 021

#3 = 011

#4 = $0\bar{1}1$

#5 = $0\bar{2}1$

#6 = $0\bar{2}\bar{1}$

#7 = $02\bar{1}$

CRYSTAL CROSS-SECTION PERPENDICULAR TO A AXIS

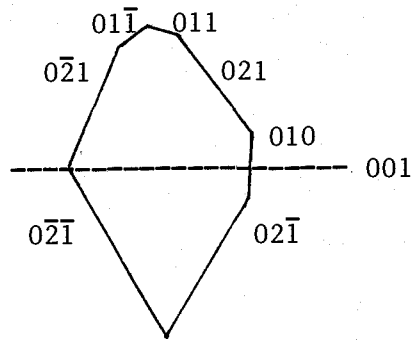

of a typical K_2SO_4 crystal with the faces assigned as to best agreement with the calculated angles.

For polarization studies it is necessary to have crystal faces perpendicular to each of the three crystallographic axes; these are the 100, 010 and 001 planes. Since these faces do not occur naturally it was necessary to prepare them artificially. The crystal is mounted such that an identified face is at the appropriate angle to the grinding surface so that the face formed by sanding will be coplanar with the desired plane. The angle between the natural face and the prepared face can be periodically measured during the grinding and polishing process to ensure that coplanarity with the desired plane is maintained. Using this technique faces were regularly prepared within 5° of the desired plane.

C. Thin K_2SO_4 Sections for I.R. Transmission

Crystal samples of K_2SO_4 for I.R. transmission were prepared with faces perpendicular to each crystallographic axis and were of various thicknesses (4-5μ up to 800μ). The cross-sectional area was typically 2 x 2 mm., but for the very thin samples these dimensions decreased to about 1/2 x 1/2 mm. Micro sampling techniques included the use of a Beckman beam condenser with KBr lenses and a rotating sample holder. A silver chloride multiple reflection polarizer was used for polarizing the incident radiation. The sample was rotated in a plane perpendicular to the light propagation to effect changes in polarization since rotating the polarizer would cause

energy losses due to cross polarization with the instrument. The Beckman I.R. 7 was used for all of the I.R. work with a NaCl fore-prism interchange for the region 650-4000cm^{-1} and a CsI interchange for the region 350-700cm^{-1}.

As previously mentioned the faces needed for spectroscopic study were not naturally occurring in the particular habit that was prevalent in crystals grown by evaporation at room temperature. Therefore, it was necessary to cut the desired faces from the available samples. A suitable sample was chosen and the orientation of the morphological faces was determined goniometrically and then the crystal was positioned against an abrasive surface such that the face formed by moving the crystal over the surface would coincide with the desired face. Coarse emery paper was used until a face of suitable dimensions was obtained. Once a face was sufficiently large for use, the sample was rotated 180° to form a face on the opposite side coplanar with the first face. The sample could then be thinned down by continuing the abrasive procedure on the second face until the desired thickness was obtained. The final thinning was done using an optical flat and carborundum powder.

The thickness could be measured with a calibrated microscope, by first focusing on the upper face and then noting the distance that the calibrated fine adjustment knob was moved in bringing the bottom surface into focus and correcting this distance by multiplying by the refractive index of the sample. Samples could be measured quite accurately down to thicknesses of 20μ, then

comparison of peak intensities was used for further measurements. When samples were produced with good coplanarity between the two faces, interference fringes could also be used for thickness measurements. For the cases that fringes were observed there was excellent agreement between the two methods.

Good spectra were attainable in the combination regions with samples of 100 -700μ and these samples could be prepared without the necessity of affixing them to a supporting substrate. The thinner samples that were prepared for the study of the fundamental regions were mounted to KBr substrates with various materials; expoxy was found to be quite free of strong absorptions in the regions of K_2SO_4 fundamentals for the thin films of adhesive required to hold the sample. Samples were taken down to 4-5μ with this method, but the fundamentals ν_3 and ν_4 were still much too intense. The other two regions ν_1 and ν_2 could, however, be studied and the components assigned using polarization.

D. Sample Preparation for I.R. Reflection and Raman

The crystals for reflection measurements had to be larger than those for transmission. A face suitable for a good reflection spectrum should be at least 1x1 cm. The faces were prepared normal to the crystallographic axes in the same way that the thin samples were prepared with the exception that sample was not thinned down as in the case of transmission.

The crystals for Raman work were prepared very similarly to those for reflection except the crystal size was much smaller. Faces 2x2 mm were acceptable for Laser Raman spectroscopy. One other difference was that the Raman samples required that not only the incident face be plane but that a face 90° from this face must also be plane and normal to a crystallographic axis.

IV. RAMAN SCATTERING OF K_2SO_4 SINGLE CRYSTALS

The Raman spectra were taken on an instrument at the University of Oregon, with the cooperation of Dr. W. Peticolas. The actual instrumental operation was performed by Mr. W. Small and Mr. G. Hibler. The instrument consisted of a Spex monochromator with a photo-cathode tube detector. A He-Ne Laser was used for the incident source utilizing the λ = 6328.17 Å lasing line. The photon counts were converted to an electrical signal and recorded on a strip-chart recorder.

The final calibration of the instrument was checked by measuring several of the less intense Ne emission lines from the laser. For this particular measurement the pre-filter on the laser beam was removed. The wavelengths, measured to the nearest half angstrom, are given in the following list along with the corresponding values from the emission spectra of Ne given in the Chemical Rubber Co. Handbook.

Measured (Å)	CRC Values (Å)
6351.5	6351.87
6382.5	6382.99
6401.0	6401.08
6410.0	6409.75
6445.0	6444.72
6506.5	6506.53
6533.0	6532.88
6599.0	6598.95
6603.5	6602.91
6667.5	6666.89
6678.5	6678.28
6717.0	6717.04
6739.0	6738.06

The standard deviation is 0.4Å, which gives an error of ± 2 cm^{-1} at 6350 Å and ± 2 cm^{-1} at 6750 Å when measuring scattering from the 6328.17 Å line.

The samples as previously described were oriented such that selective polarizations of the incident radiation upon faces normal to the crystallographic axes could be used to determine relative polarizations of the various Raman allowed scattering. The spectra of K_2SO_4 showed several components of lattice modes in the low frequency region and components of the characteristic internal vibrations of the sulfate ion in the region from 450-1150cm^{-1}.

Spectra were taken with the incident beam parallel to the three symmetry axes and with the scattered light also parrallel to the axes. The incident radiation had a fixed polarization while the scattered radiation could be polarized normal to or parallel to the direction of the incident beam.

Spectra were obtained from three different sample orientations with two analyzing polarizer positions each. Each spectrum is representative of the scattering arising from one of the six components of the polarizability tensor. By comparing the results of the six spectra the specific polarization of each component can be determined.

In order to define a particular experimental arrangement the following symbol will be used:

$$1(k\ j)i$$

i = incident direction
j = incident polarization
k = scattered polarization
l = scattered direction

Therefore, z(xx)y describes a situation in which the laser beam is directed perpendicular to the 010 face with x polarization. The radiation scattered in the z direction is analyzed under x polarization. By simply rotating the analyzing polarizer 90° the arrangment becomes z(yx)y. The letters in the parentheses represent the particular term of the polarizability tensor that is Raman allowed by the particular arrangment.

The following figures show the results of the spectral measurements with each figure representing one crystal orientation and the resulting two polarizations obtained by use of the analyzing polarizer. Since the sample remained fixed in the beam between the two polarizations the relative intensities of the two spectra are meaningful. The relative intensities between the three figures, however, cannot be used since there was no attempt to standardize the intensity of the scattered radiation when various crystal orientations were made.

Figures 5, 6, and 7 give the spectra of the lattice vibrational region and Figures 8, 9, and 10 give the spectra arising from the fundamental vibrational modes.

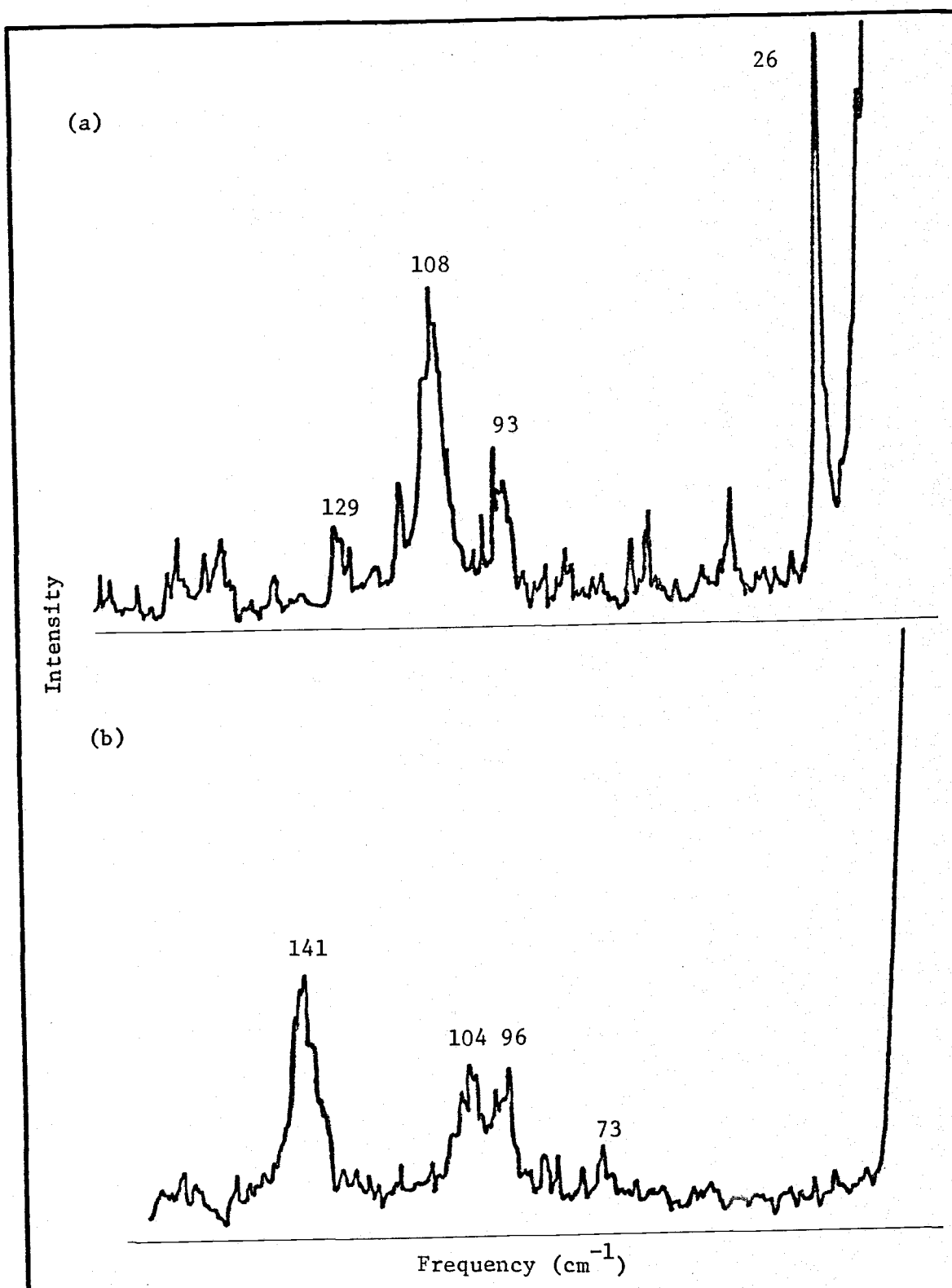

Figure 5. Raman Spectra of the lattice mode region of K_2SO_4 crystals, (a) α_{xx} components, (b) α_{xy} components

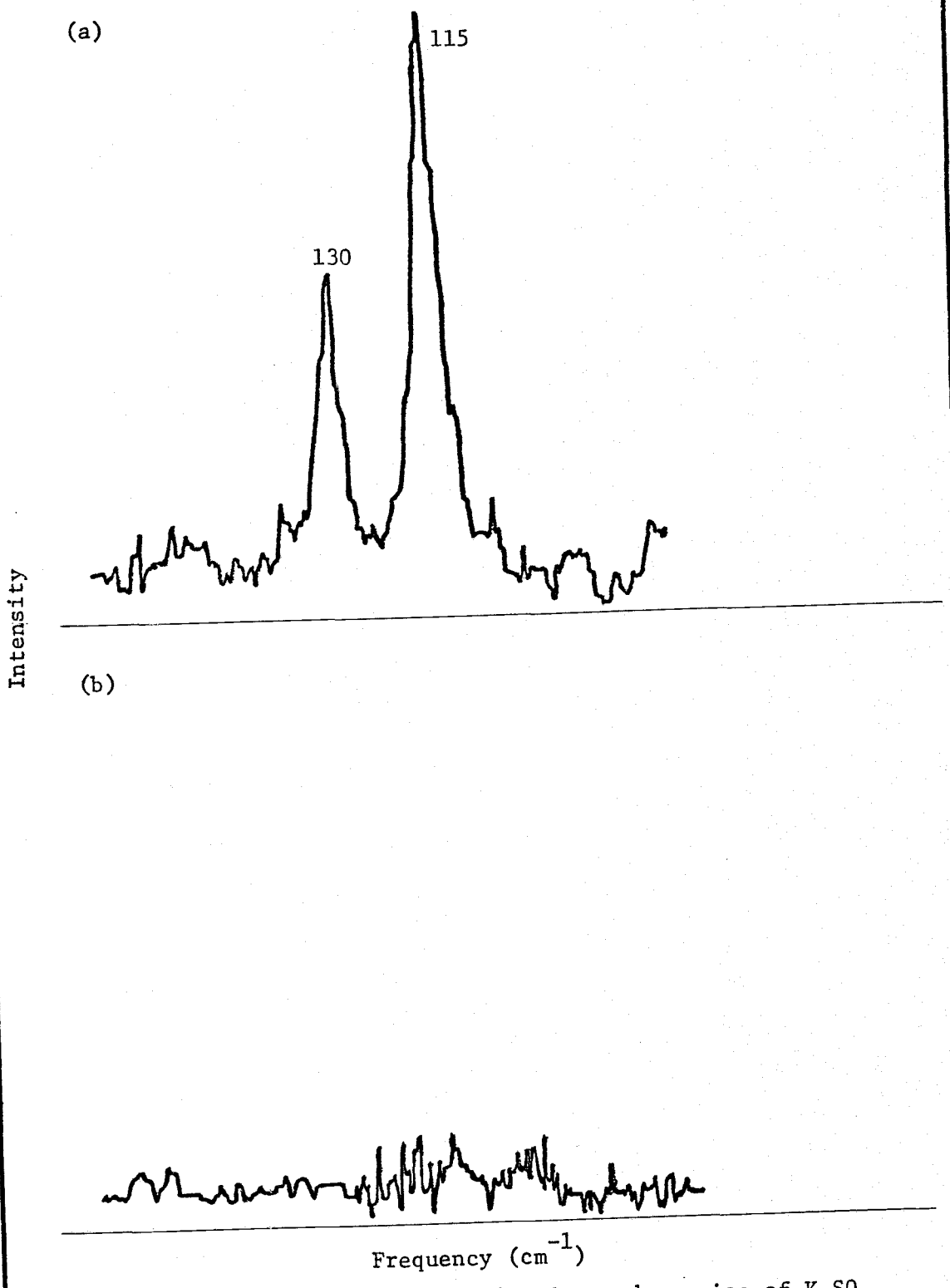

Figure 6. Raman Spectra of the lattice mode region of K_2SO_4 crystals, (a) α_{yy} components, (b) α_{yz} components

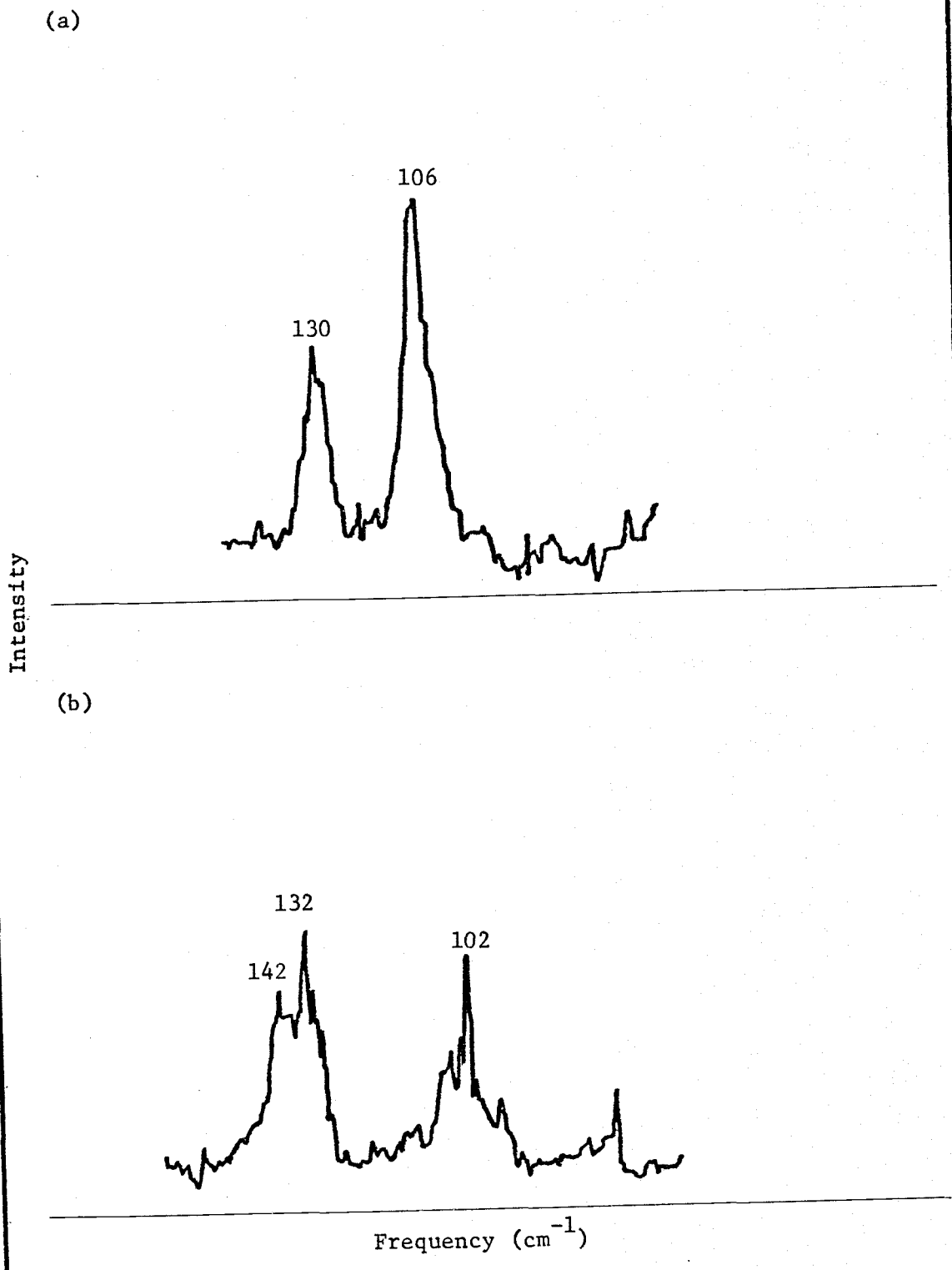

Figure 7. Raman Spectra of the lattice mode region of K_2SO_4 crystals, (a) α_{zz} components, (b) α_{xz} components

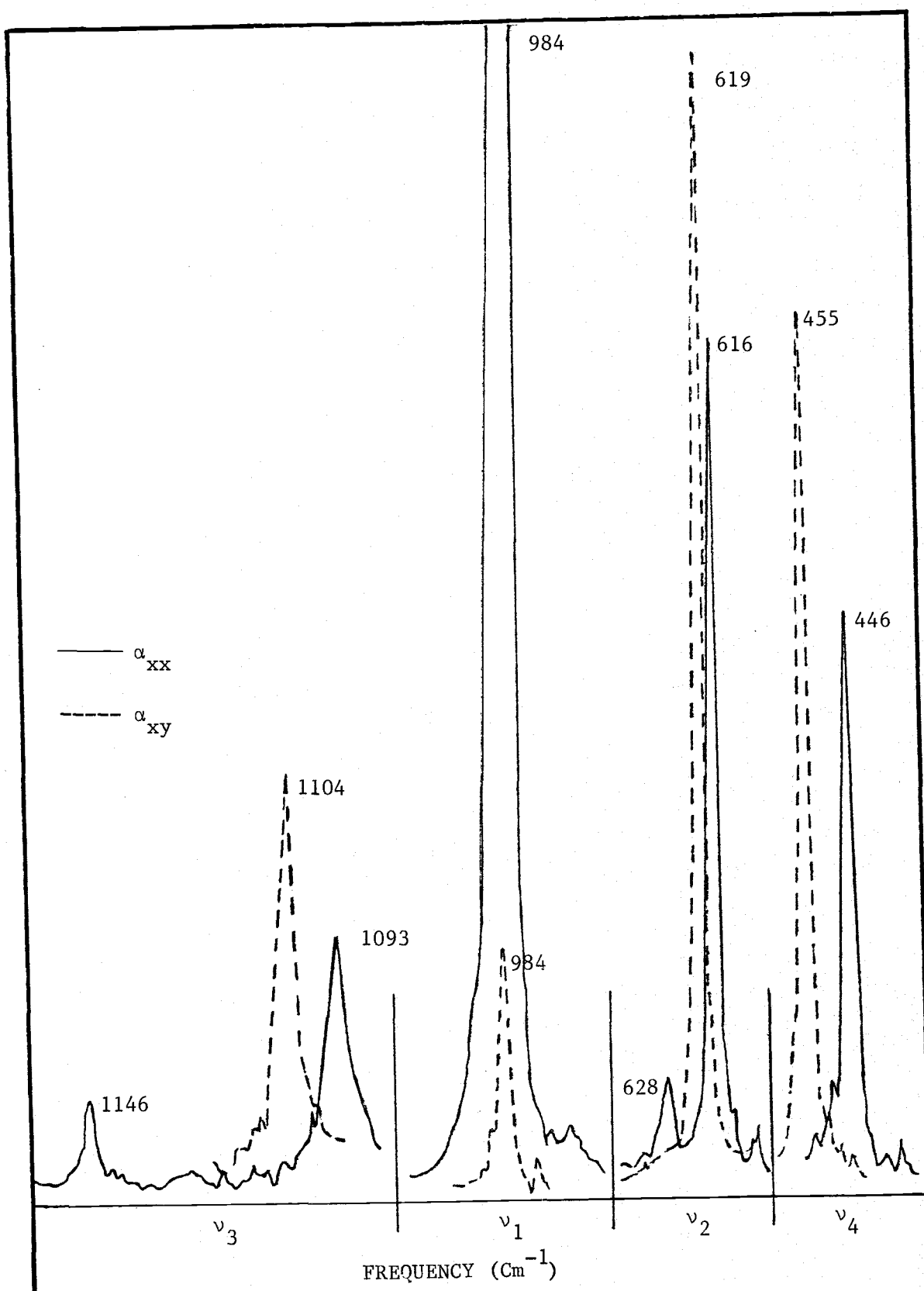

Figure 8. Polarized Raman spectra of K_2SO_4 showing the sulfate ion stretching fundamentals

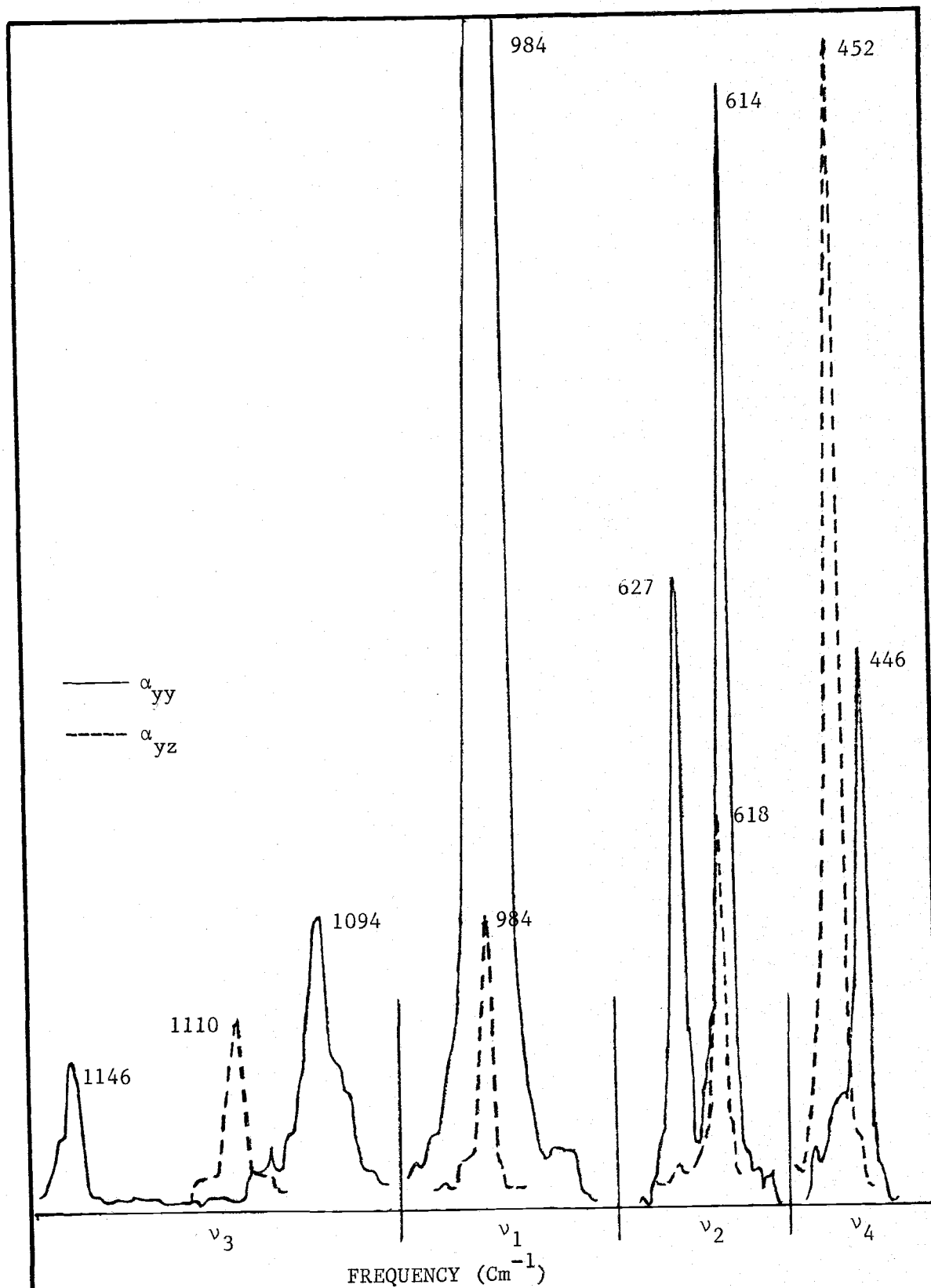

Figure 9. Polarized Raman spectra of K_2SO_4 showing the sulfate ion stretching fundamentals

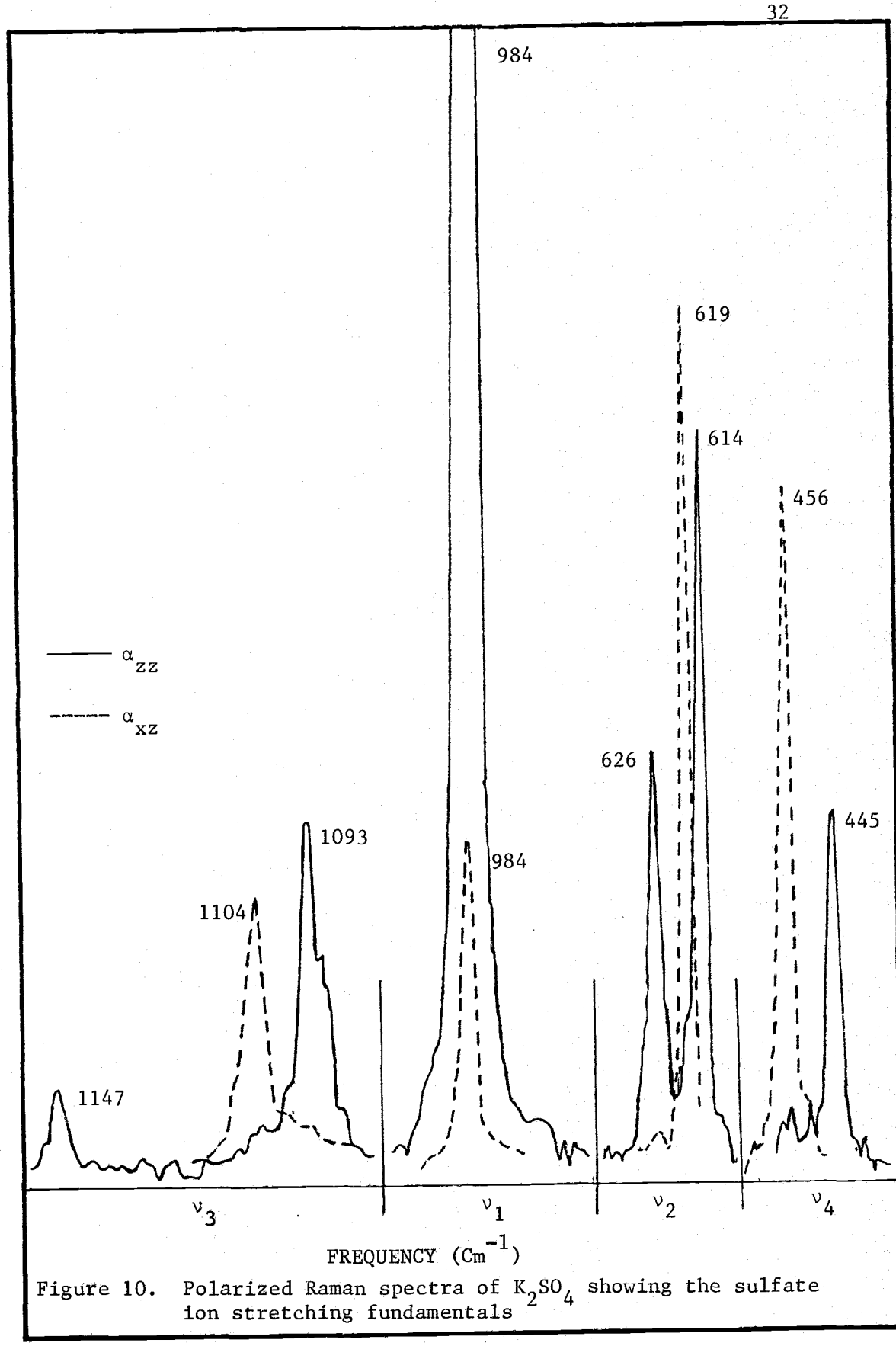

Figure 10. Polarized Raman spectra of K_2SO_4 showing the sulfate ion stretching fundamentals

A. DISCUSSION OF RAMAN RESULTS

The internal vibrations of the sulfate ion are responsible for the peaks occurring above 400 cm^{-1}. The free $SO_4^{=}$ has T_d symmetry and has four fundamental frequencies associated with it, a totally symmetric mode near 983 cm^{-1}; a doubly degenerate mode near 458 cm^{-1} and two triply degenerate modes near 620 cm^{-1} and 1105 cm^{-1}. These frequencies are assigned the following symmetry species under T_d symmetry, ν_1 (983 cm^{-1}) is an A_1 type mode, ν_2 (458 cm^{-1}) is an E, and ν_3 (1105 cm^{-1}) and ν_4 (620 cm^{-1}) are F_2 symmetry species.

Since, as previously stated, the sulfate ion occupies a site in the lattice of symmetry lower than C_3, the degenerate modes will have their degeneracies lifted. Another possible cause for splitting arises from the intermolecular coupling which can occur when the unit cell contains more than one molecule and in this case there are four molecules. The predicted splittings are conveniently shown by the use of the following correlation diagram:

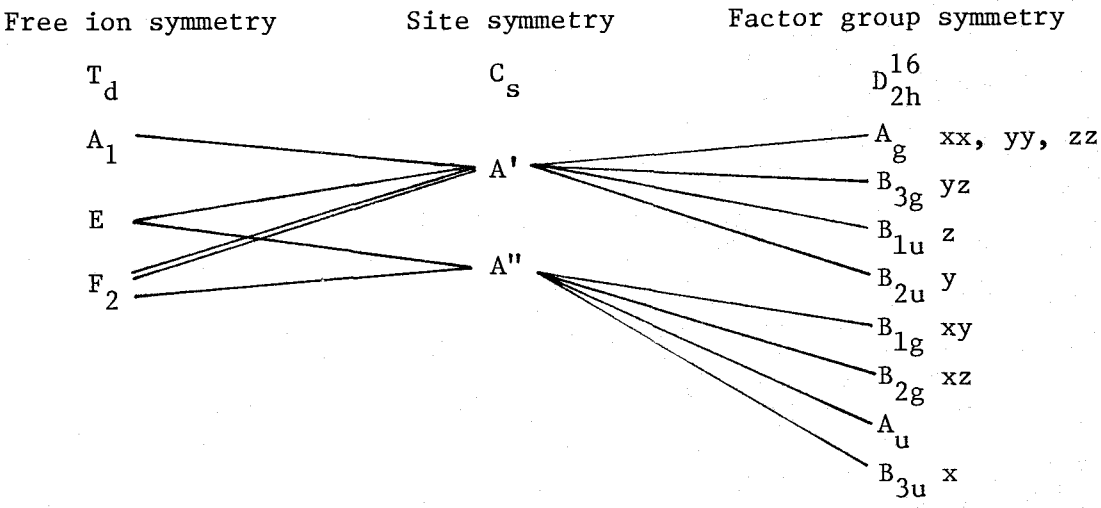

Table 6 shows the Raman emissions for the lattice region and the fundamental regions. The polarization is indicated by using the appropriate term of the polarizability tensor.

From the diagram the lifting of all degeneracies is predicted by the site effect and each of these components would be further split into four distinquishable frequencies depending upon the magnitude of the intermolecular coupling. A thorough investigation of the I.R. absorptions as well as the Raman spectra should lead to a prediction of the extent of coupling by determining the number, as well as, the polarization of absorptions in the fundamental regions. A full interpretation of the data will be postponed until the I.R. data has also been presented.

Table 6. Raman values for the lattice modes and internal sulfate fundamentals of single crystalline K_2SO_4

This Work			V. Ananthanarayanan	
Mode	Frequency (cm^{-1})	Polarization*	Mode	Frequency (cm^{-1})
	26	xx		54
	73	xy		73
				85
	93	xx		92
	96	xy		
	102	xz		
	014	xy		
	106	zz		107
Lattice	108	xx	Lattice	
	115	yy		
	129	xx		
	130	yy,zz		131
	132	xz		
	141	xy		140
	142	xz		
				160
	445	zz		
	446	xx,yy		447
	452	yz		
ν_2	455	xy	ν_2	455
	456	xz		
	614	yy,zz		
	616	xx		
	618	yz		
ν_4	619	xy,xz	ν_4	620
	626	zz		
	627	yy		
	628	xx		628
ν_1	984	xx,yy,zz	ν_1	985
	1093	xx,zz		1092
	1094	yy		
ν_3	1104	xy,xz	ν_3	
	1110	yz		1108
	1146	xx,yy		1146
	1147	zz		

*Expressed as subscripts of the polarizability tensor term.

V. REFLECTION MEASUREMENTS OF K_2SO_4

A. EXPERIMENTAL DISCUSSION

The reflectance measurements were carried out on a Beckman I.R. 7 spectrophotometer with special apparatus to change from the normal transmission arrangement. Reflection of the incident radiation from the surface of the crystals was taken at various angles of incidence. The near-normal incident reflection measurements were accomplished with the use of a standard reflection apparatus with a gold-grid polarizer used to produce the polarized incident radiation.

The non-normal incident reflection measurements were obtained using a modified mirror beam condenser, Barnes Beam Condenser, Model 128. With the plane mirror of the condenser removed, the sample was mounted in its place with its surface coplanar with the original position of the plane mirror. Polarization was accomplished by means of a silver chloride multiplate reflection polarizer.

Two non-normal incident reflection arrangements are to be distinguished. One type, referred to as TM mode of reflection, has the electric vector of the incident radiation in the plane of incidence. Thus the electric vector in the TM case has a component parallel to the incident face and a component perpendicular to the surface. This allows the possibility of interaction with

the radiation in both the transverse and the longitudinal directions. The second kind of arrangement, known as TE mode of reflection, has the electric vector of the incident radiation normal to the plane of incidence and hence can give rise only to coupling with the transverse phonons since the electric vector can only be parallel to the surface since the plane of incidence is perpendicular to this surface.

The TM measurements were made with the apparatus in a horizontal arrangement, which would be the normal position when used as a beam condenser for transmission work, with the polarizer fixed for horizontal polarization. In order to make the TE measurements, however, the sample supporting apparatus was rotated 90° into a vertical position and the polarizer remained fixed. Simply rotating the polarizer would have resulted in cross polarization with the instrument and consequently a loss of energy. Since the sample size was not large and reflection alignment was difficult this afore-mentioned loss of energy represented a situation incompatible with the sensitivity of the instrument. Therefore, as mentioned, the beam condenser unit was supported in the vertical poistion with the concave mirrors also rotated 90° on their supports which put them into the same relative position as they were prior to rotating the unit. The light path now, however, was diverted vertically from its original path onto the sample, reflected, and diverted again into the instrument.

The two spectral regions studied by reflection were 590 - 630 cm^{-1} and 1080 - 1200 cm^{-1}, corresponding to the internal vibrational modes ν_4 and ν_3, respectively, of the sulfate ion.

The main objective in studying these reflection spectra was to obtain frequencies for the transverse limit of the components of each band which, according to Born and Huang (4), would correspond to the frequencies of the maximum absorptions in the limit of very thin films. Several methods exist for obtaining the optical constants from the reflection data. The absorption coefficient could then be plotted versus frequency to obtain the desired frequencies of the absorption maxima. One such method is based on a set of Kramers-Kroning relations (3), one of which is:

$$\varepsilon_1(\omega)-1 = \frac{2}{\pi} P \int_0^\infty \frac{x\varepsilon_2(x)dx}{x^2-\omega^2} \qquad (1)$$

where ε_1 = the real part of the dielectric constant at the particular frequency, ω.

P = the principal part at $x = \omega$

ε_2 = the imaginary part of the dielectric constant as a function of frequency.

In order to use this technique, however, absolute intensities for the band of interest as well as those in regions quite distant from the absorbing region must be known quite accurately. This work made no attempt to meet these requirements as the optical constants were not the objective of the measurements.

It has been shown (12) from calculated reflection spectra of calcite that the inflection point on the low frequency side of a

a reflection band seemingly corresponds to ν_T and is fairly invariant over various incident angles of reflection. This work tends to substantiate these findings.

B. EXPERIMENTAL OBSERVATIONS

The near-normal (0-6°) reflection bands of Figures 11 and 12 for ν_4 and ν_3, respectively, show quite different features depending upon which axis was chosen parallel to the polarized electric vector. The convention used was to designate a particular band according to the axis that coincided with the electric vector with the crystallographic unit vector a corresponding to the cartesian coordinates x, b to y, and c to z. Therefore, for the x-polarized measurements, for example, the reflection arises from a large value of the absorption coefficient due to the x component of the transverse type phonon mode. The inflection point on the low frequency side of this reflection band is then taken as the value for the frequency of the absorption maximum of the x component for transmission in the limit of a very thin film. The y and z components are similarly obtained for the lower frequency part of the band. Since both bands seemed to be composed of at least two constituents the lower frequency side of the higher frequency components were extrapolated far enough to allow an estimate for the ν_T of the components. The values obtained from these measurements are presented in Tables 7 and 8.

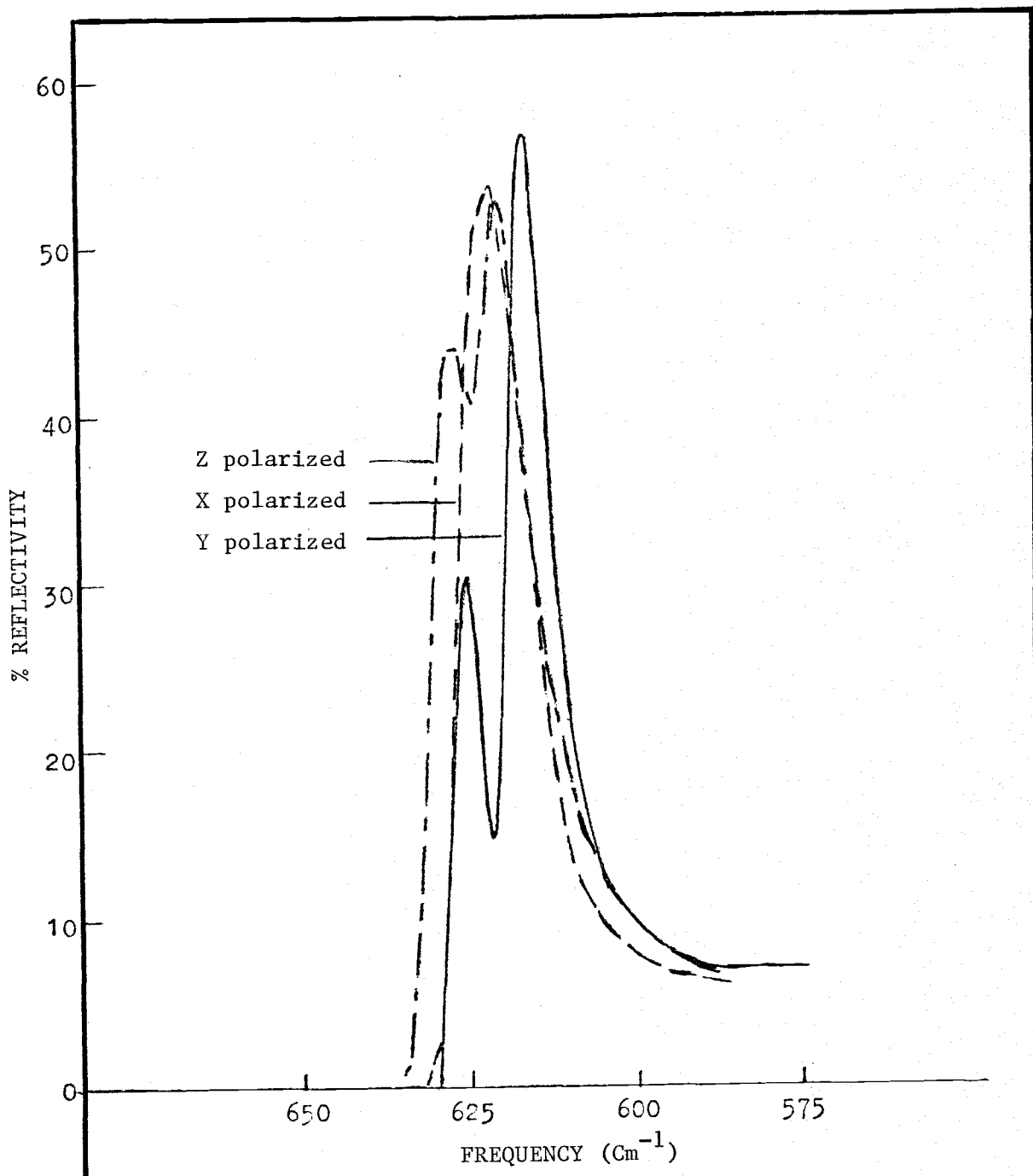

Figure 11. Polarized I.R. reflection spectra at near normal incidence of the sulfate ion ν_4 region

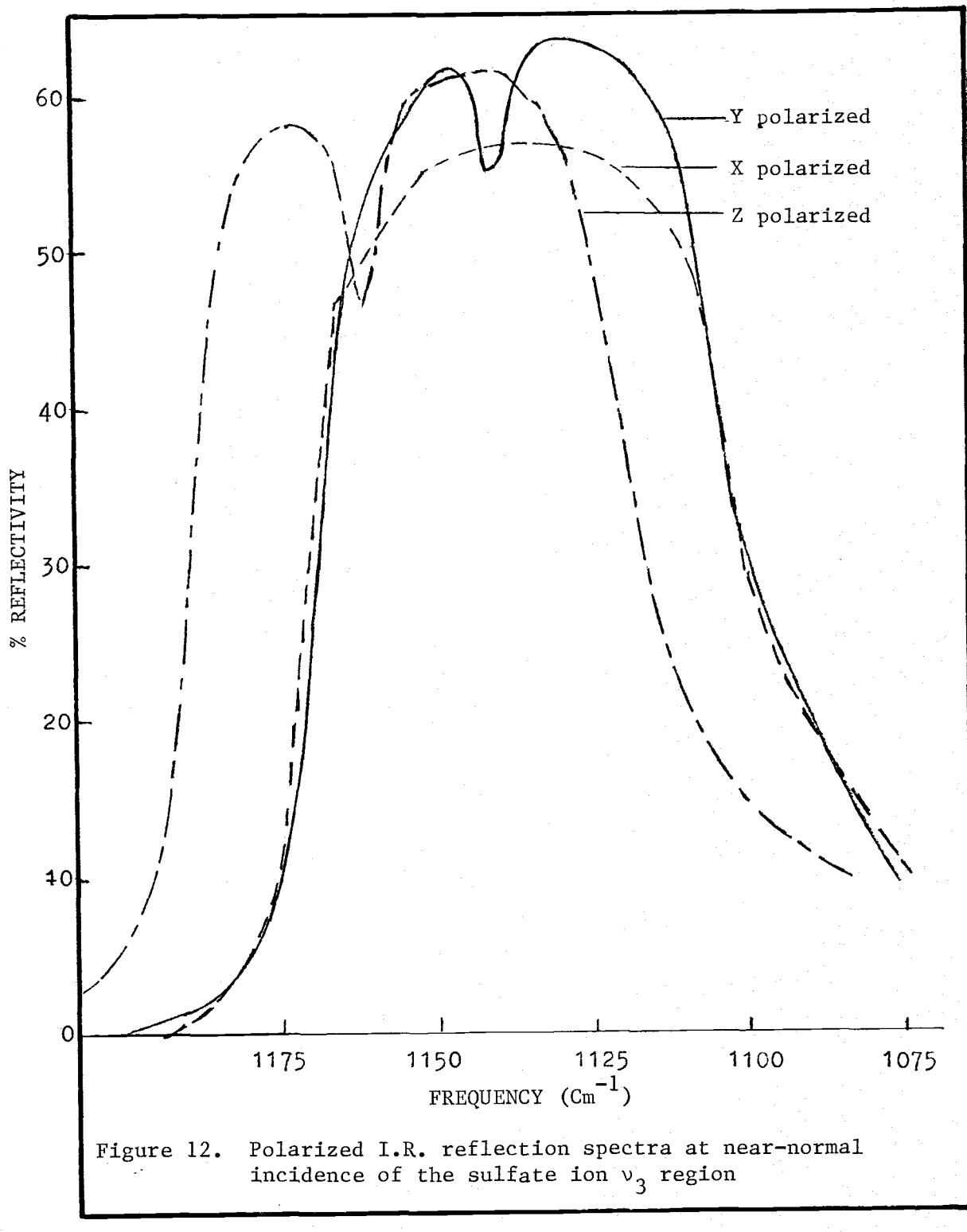

Figure 12. Polarized I.R. reflection spectra at near-normal incidence of the sulfate ion ν_3 region

Table 7. Values of ν_T and ν_L for three angles of reflection in the ν_3 region

Low Frequency Inflection Points (ν_T)

Polarization	Near-Normal	38°		52.5°			
	(cm^{-1})	T_M (cm^{-1})		T_M (cm^{-1})		T_E (cm^{-1})	
x	1104.5	1107.5	(xz)*	1107	(xz)	11-4	(yz)
		1106	(xy)	1105	(xy)		
y	1106	1107.5	(yz)	1108	(yz)	1108	(xz)
	1104**	1104	(xy)	1104	(xy)		
z	1121	1123	(xz)	1123	(xz)	1121	(xy)
	1162**	1123.5	(yz)	1122	(yz)		

High Frequency Inflection Points (ν_L)

Polarization	Near-Normal	38°		52.5°			
	(cm^{-1})	T_M (cm^{-1})		T_M (cm^{-1})		T_E (cm^{-1})	
x	1172.5	1182	(xy)	1192	(xy)	1197.5	(yz)
		1192	(xz)	1195	(xz)		
y	1168.5	1177.5	(xy)	1187	(xy)	1194	(xz)
		1190	(yz)	1191.5	(yz)		
z	1190	1201.5	(yz)	1211.5	(yz)	1211	(xy)
		1201	(xz)	1212	(xz)		

*Plane of incidence.
**Estimated by extrapolation.

Table 8. Values of ν_T and ν_L for two angles of reflection of the ν_4 region

Low Frequency Inflection Points (ν_T)

Polarization	Near-Normal	52.5°	
	(cm^{-1})	T_M (cm^{-1})	T_E (cm^{-1})
x	616.5	616 (xy)*	615 (yz)
		617 (xz)	
y	613	613 (xy)	613 (xz)
		613.5 (yz)	
	623	623 (yz)	622.5 (xz)
		623.5 (xy)	
z	617	617.5 (xy)	618 (xy)
		618 (yz)	
	623**		624 (xy)

High Frequency Inflection Points (ν_L)

Polarization	Near-Normal	52.5°	
	(cm^{-1})	T_M (cm^{-1})	T_E (cm^{-1})
x	627	627.5 (xz)	620 (yz)
		629.5 (xy)	
y	618.5	618 (xy)	618.5 (xz)
		618 (yz)	
		628 (xy)	628.5 (xz)
z		624 (yz)**	625 (xy)**
		624.5 (xz)	
	631	632 (yz)	633.5 (xy)
		633 (xz)	
		634.5 (xz)	
		634.5 (yz)	

*Plane of incidence.
**Estimated by extrapolation.

The reflection measurements from the non-normal incident experiments were taken at two angles for the ν_3 region, namely 38° and 52.5° from normal incidence, and at 52.5° only for the ν_4 region. In all the 52.5° incident measurements both TM and TE spectra are made, but only TM measurements were made at 38° incidence.

When the sample is oriented in the non-normal incident apparatus such that the electric vector is perpendicular to the plane of incidence with, for example, the reflecting surface the 010 face, the angle of incidence 52.5°, and the electric vector parallel to the x direction in the crystal, the following notation is used:

$$TE(010,\ 52.5°,\ X_T)$$

A similar notion of TM arrangements gives the plane of the reflecting surface, the angle of incidence, direction of the component of the electric vector in plane of the incident surface, and, in addition, the direction of the component of the electric vector perpendicular to incident surface, such as:

$$TM(001,\ 52.5°,\ X_T,\ Z_L)$$

The reflection data for ν_3 taken at 52.5° incidence are shown in Figures 13-15. Each set of spectra are arranged so that the low frequency inflection point arises from the same transverse component in each of the three spectra in each figure. This allows a direct

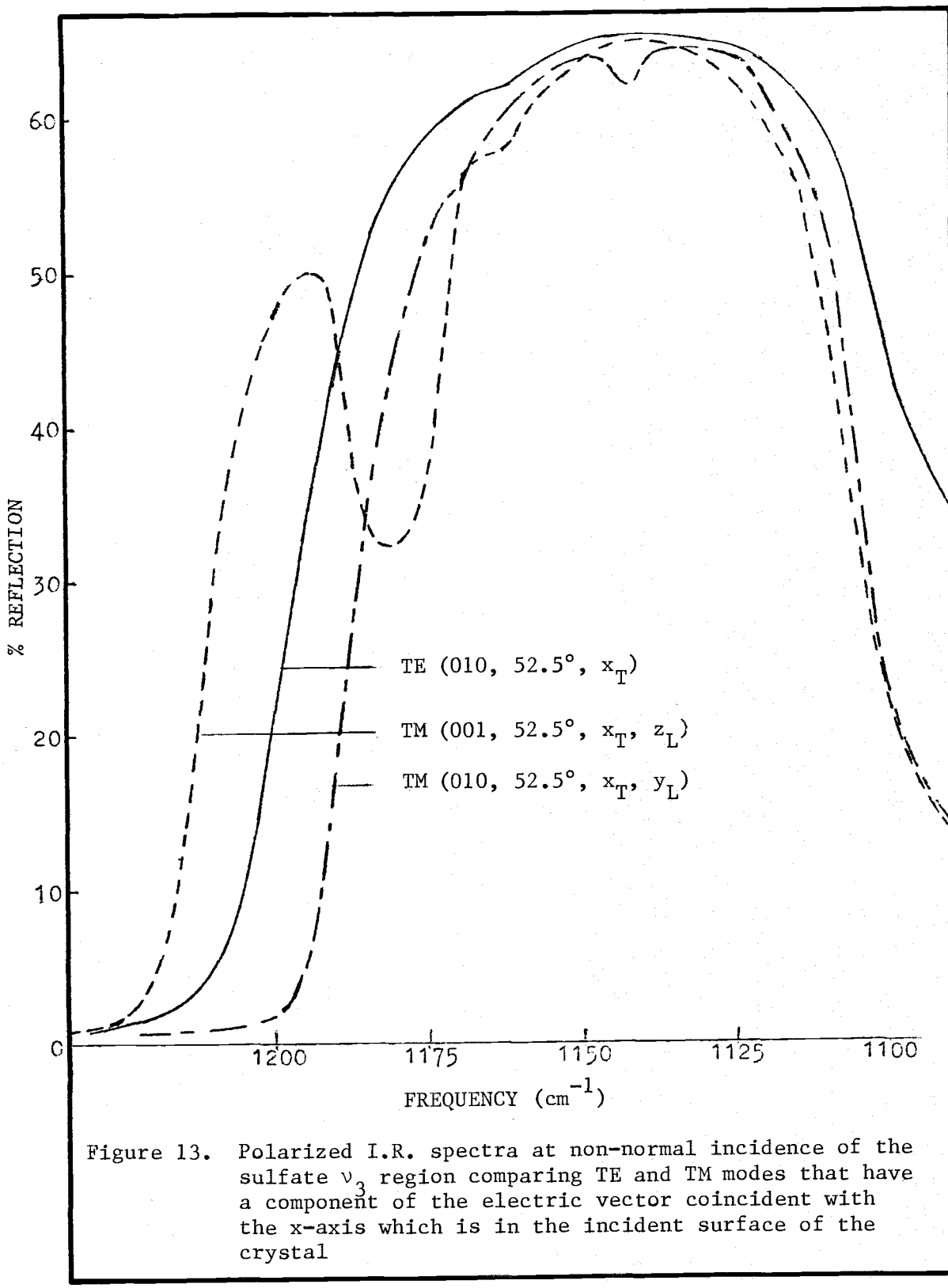

Figure 13. Polarized I.R. spectra at non-normal incidence of the sulfate ν_3 region comparing TE and TM modes that have a component of the electric vector coincident with the x-axis which is in the incident surface of the crystal

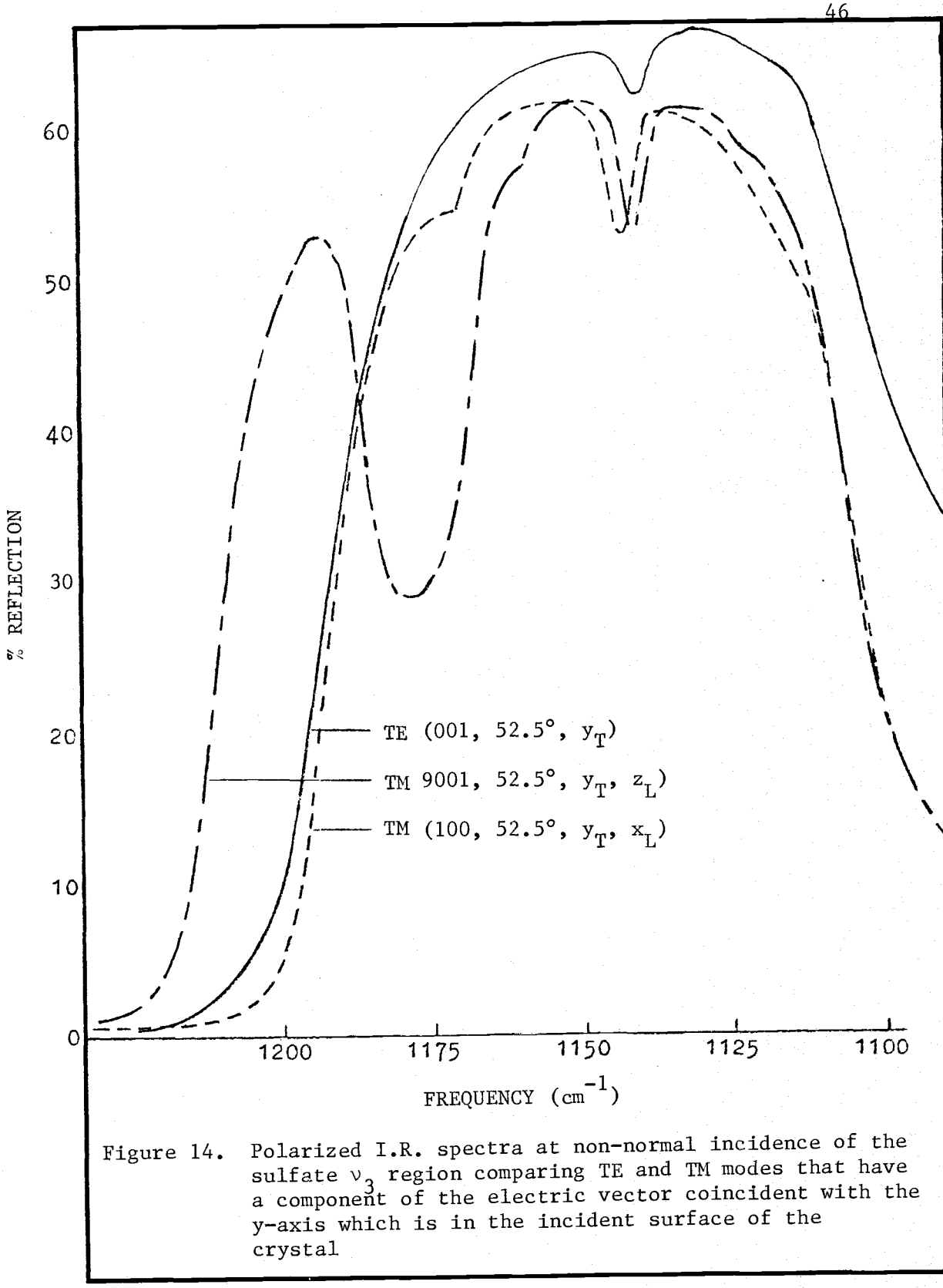

Figure 14. Polarized I.R. spectra at non-normal incidence of the sulfate ν_3 region comparing TE and TM modes that have a component of the electric vector coincident with the y-axis which is in the incident surface of the crystal

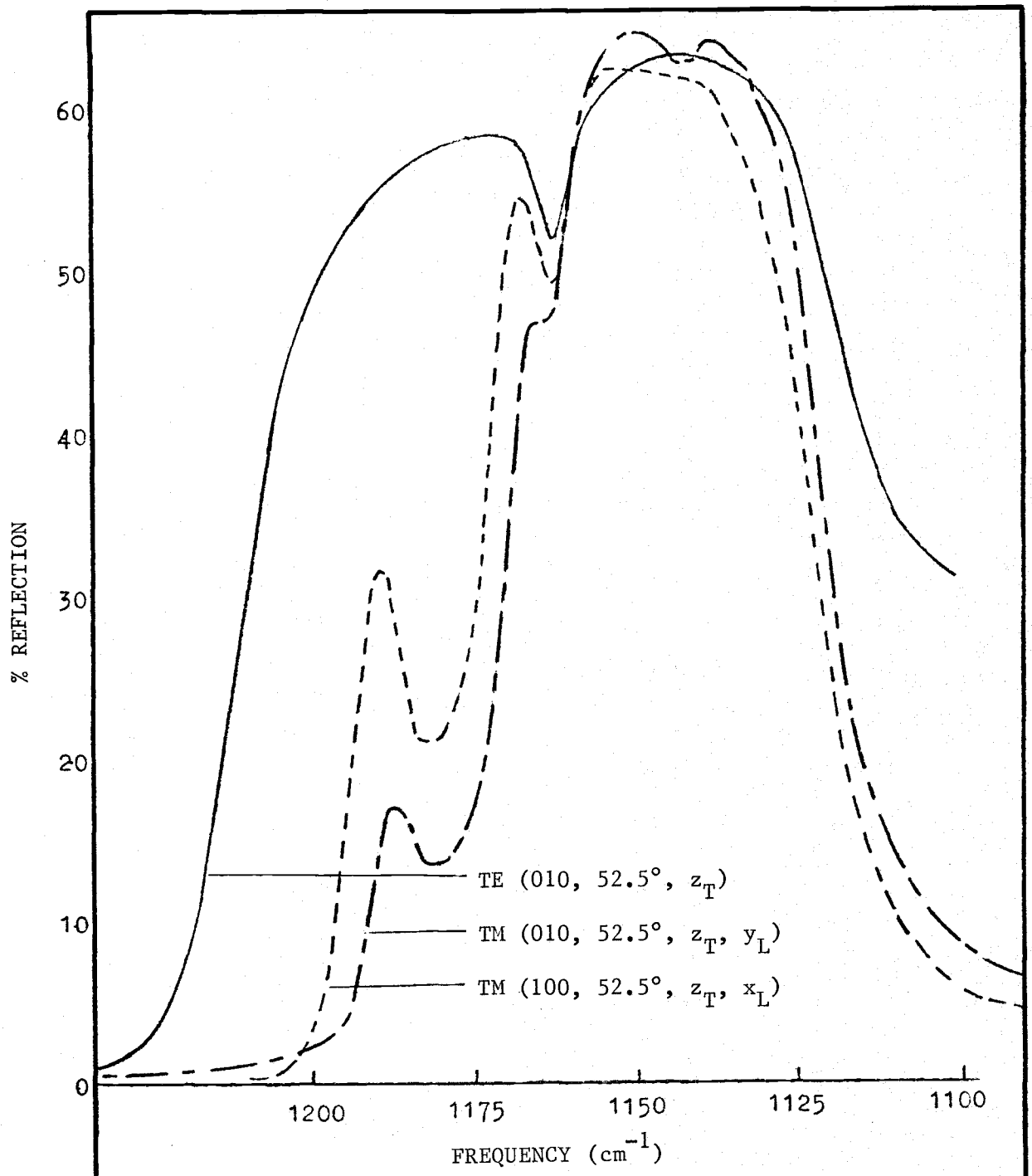

Figure 15. Polarized I.R. spectra at non-normal incidence of the sulfate ν_3 region comparing TE and TM modes that have a component of the electric vector coincident with the z-axis which is in the incident surface of the crystal

comparison of the higher frequency components arising from the longitudinal phonon modes in the TM measurements with the strictly transverse nature of the TE measurements. From Table 7 the values of ν_T from the TE reflections at 52.5° incidence agree quite well with those obtained from the near-normal spectra. The values of ν_T from the TM spectra give values slightly different from those obtained by the previous two methods, but generally within the 2 cm^{-1} range of the error introduced by methods of measuring the inflection point and the 1 cm^{-1} instrumental resolution of the reflection spectra.

A strong feature observed in Figures 13 and 14 appears to be the high frequency component due to the coupling of the longitudinal phonon mode with the z component of the incident radiation. The presence of these longitudinal features along with an apparent narrowing of the ν_T, ν_L separation distinguish the TM from the TE measurements.

For this angle of reflectance the longitudinal limit for the transverse electric vector, z_T, and for the longitudinal electric vector, z_L, agree quite well. There is less agreement for the other two directions, but this may be due to the distorting effect of more than one band in a given region. The z component seems to be of high enough frequency to be well separated from the other reflection bands.

Figures 16 through 18 show what appears to be an almost complete loss of intensity of the higher frequency z component for both

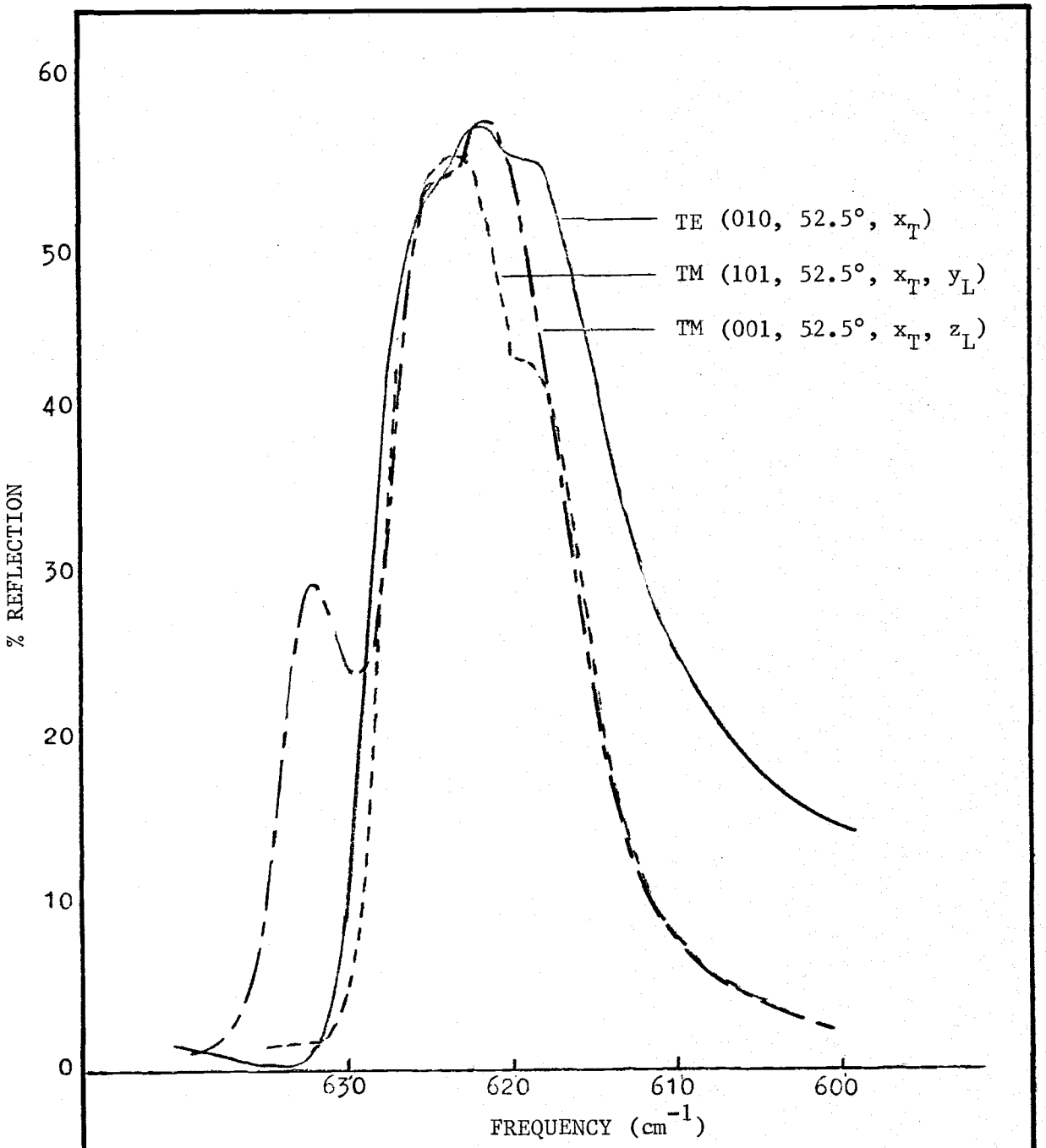

Figure 16. Polarized I.R. spectra at non-normal incidence of the sulfate ν_4 region comparing TE and TM modes that have a component of the electric vector coincident with the x-axis which is in the incident surface of the crystal

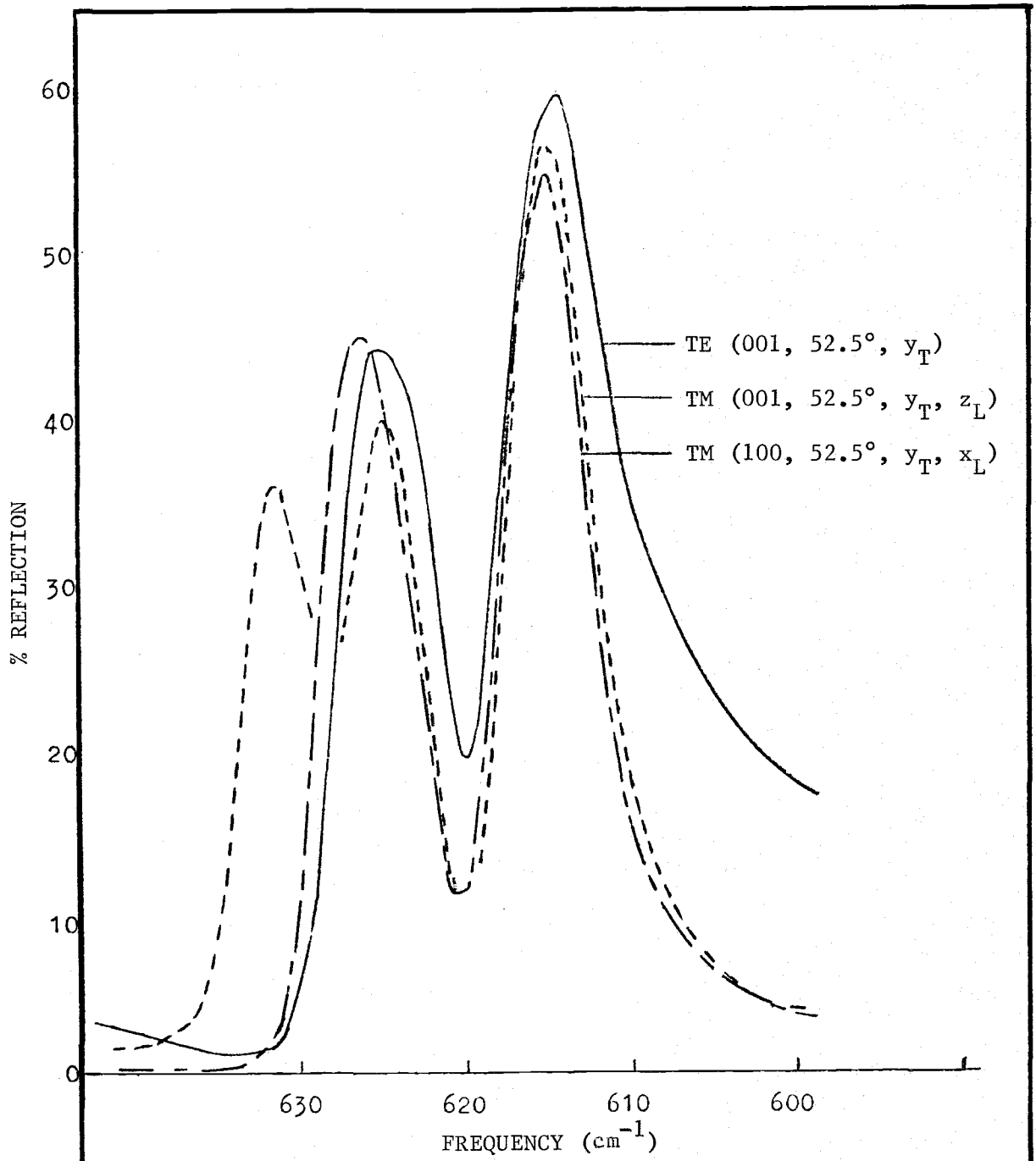

Figure 17. Polarized I.R. spectra at non-normal incidence of the sulfate ν_4 region comparing TE and TM modes that have a component of the electric vector coincident with the y-axis which is in the incident surface of the crystal

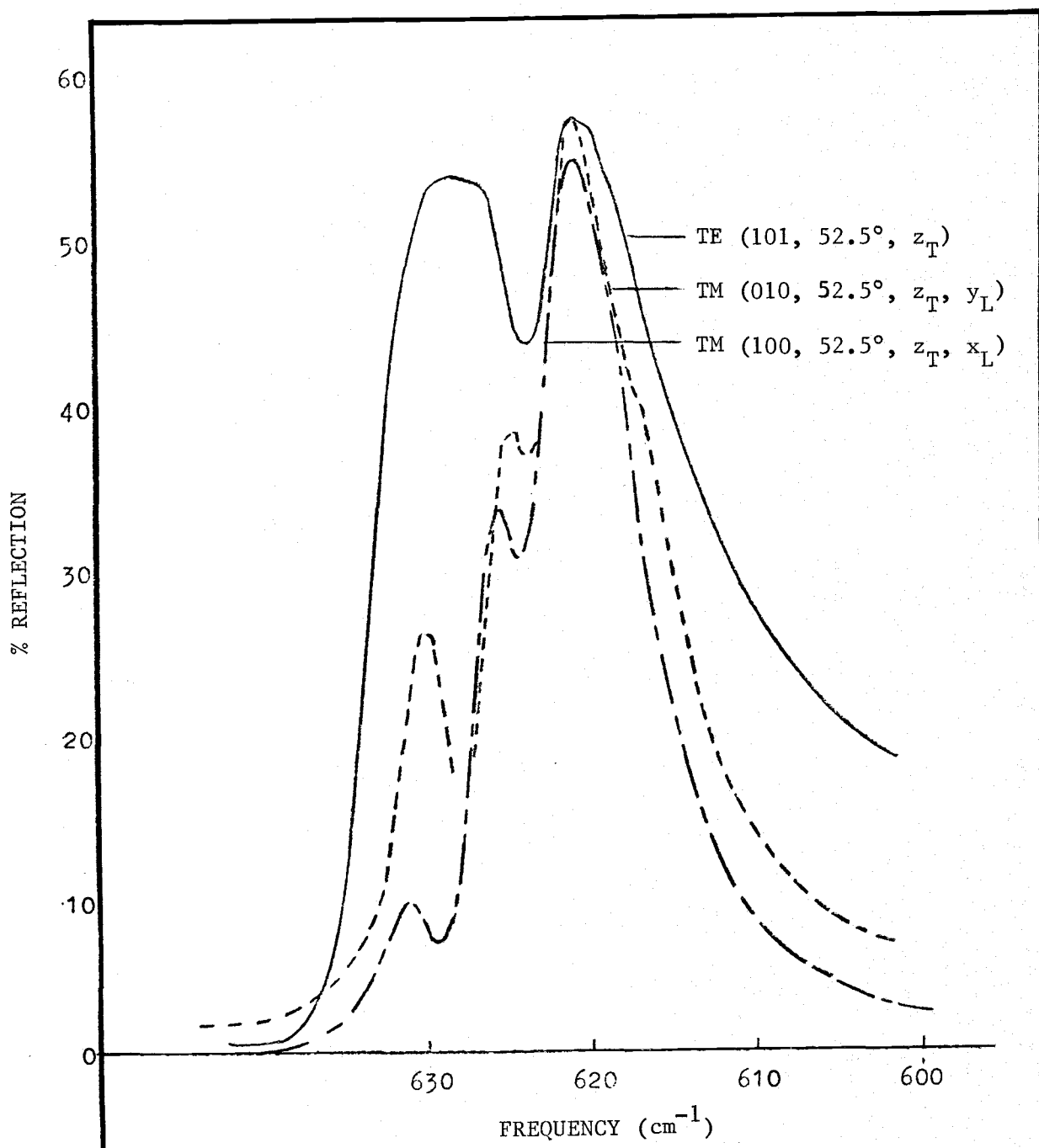

Figure 18. Polarized I.R. spectra at non-normal incidence of the sulfate ν_4 region comparing TE and TM modes that have a component of the electric vector coincident with the z-axis which is in the incident surface of the crystal.

ν_3 and ν_4. This may be accounted for by assuming that the component separations have diminished to such an extent that the entire transverse contribution of z in the TM spectra lies under the low frequency component of the TE spectra. There may well be, however, a true loss of intensity in the case of the high frequency component which is as yet unexplained.

The spectra of the ν_4 region at 52.5° follow almost identical patterns as observed for the ν_3 region. One exception is, however, the better separation of components in the y and z spectra as compared to that of ν_3. Another difference is found in the variation of the longitudinal limit, the values of ν_4 vary only slightly from near-normal measurements to the 52.5° incidence. This was not the case in the ν_3 region. The near-normal values were the lowest with the 52.5° incident values being about 20 cm^{-1} higher.

The last set of spectra, Figures 19, 20, and 21, for the reflection measurements were taken at 38° incidence in the ν_3 region. Only the TM orientation could be achieved at this angle due to the limitations of the apparatus. These spectra were very similar to the 52.5° spectra with only a little difference in relative intensities of some of the components common to the two sets of experiments. As seen in Table 7 the ν_T values for the 38° incident measurements were on the order of 10 cm^{-1} lower than the corresponding 52.5° values.

Generally, there seemed to be only minor variations with a change of the angle of incidence. The major feature being the two

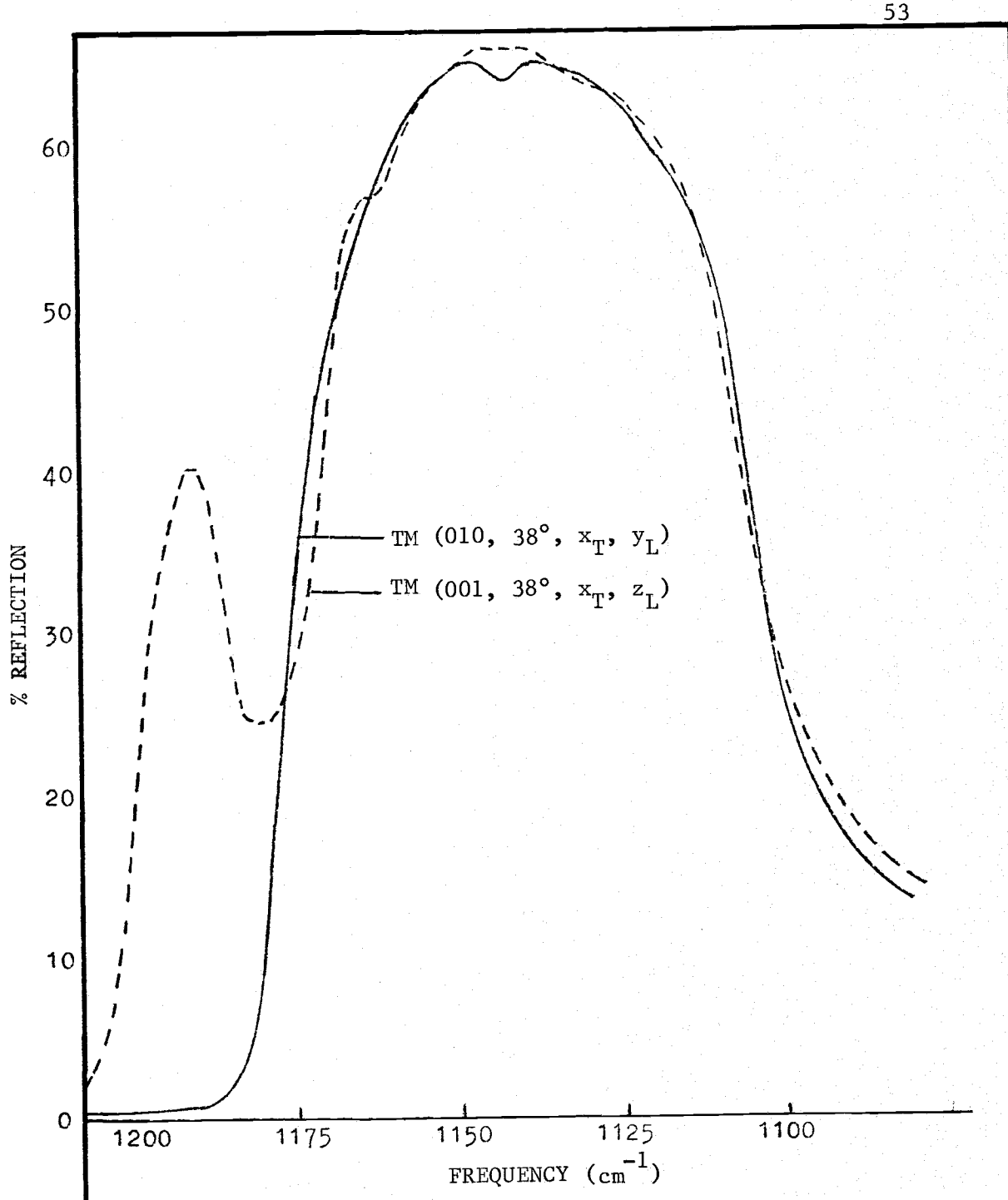

Figure 19. Polarized I.R. spectra at 38° incidence of the sulfate ν_3 region of the TM type orientation with a component of the electric vector coincident with the x-axis in common between the two absorptions

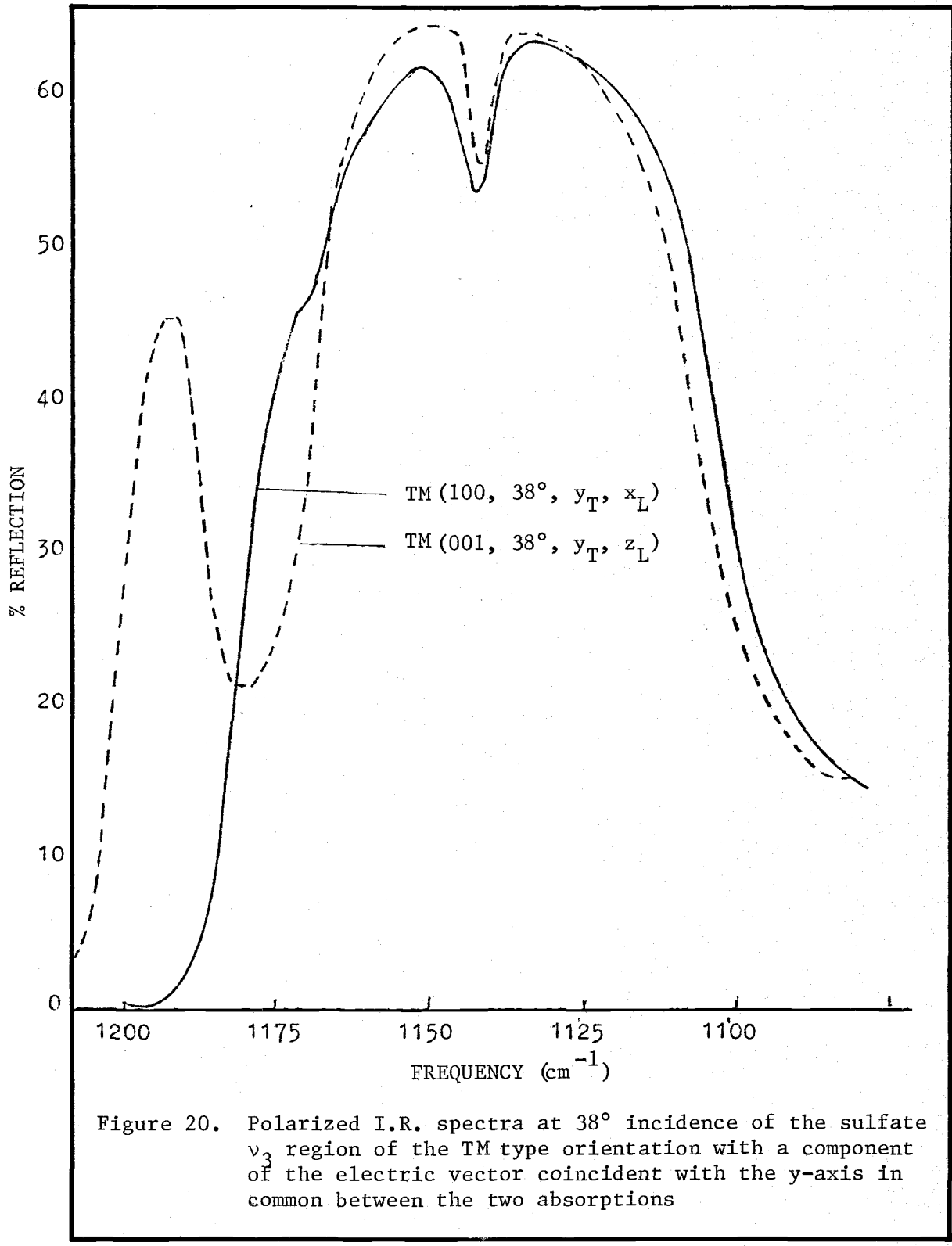

Figure 20. Polarized I.R. spectra at 38° incidence of the sulfate ν_3 region of the TM type orientation with a component of the electric vector coincident with the y-axis in common between the two absorptions

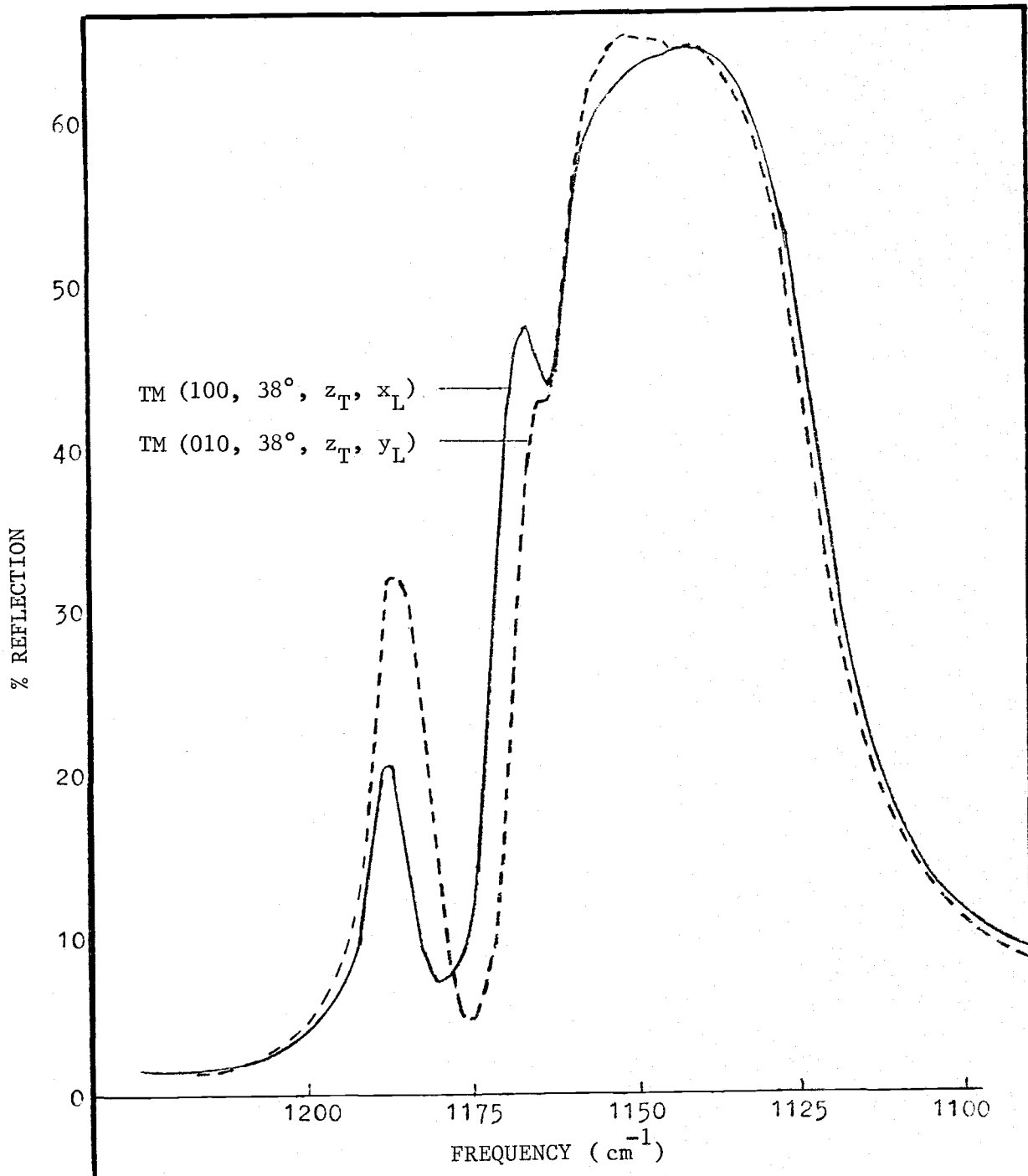

Figure 21. Polarized I.R. spectra at 38° incidence of the sulfate ν_3 region of the TM type orientation with a component of the electric vector coincident with the z-axis in common between the two absorptions

unique orientations introduced when going from normal reflectance measurements to non-normal incidence.

The ν_T assigned for ν_3 and ν_4 will be those values obtained from the near-normal spectra since these are quite representative of all the various measurements. These values will then be used when comparing the I.R. transmission and reflection data to the Raman data.

C. THEORY OF REFLECTION FROM AN ABSORBING, BIAXIAL CRYSTAL

The reflection of incident electromagnetic radiation from the surface of a crystal is dependent on several factors. These include the nature of the crystalline material, the condition of the reflecting face, the crystal dimensions and the polarization, angle and frequency of the incident radiation. The objective of this section is to present a theoretical description of the incident angle and frequency dependence of the reflectivity measurements from a specific absorbing, biaxial crystal.

In the previous section the reflection spectra are shown at several orientations for the ν_3 and ν_4 regions of K_2SO_4 crystals. A specific crystal arrangement with respect to the polarization of the incident radiation will be presented here and these results will be compared to the experimental observations.

The sulfate ν_3 and ν_4 vibrational regions of the K_2SO_4 crystal each consist of five infrared-active components whose frequencies

are not widely separated. Two of these components are x-polarized, two are y-polarized and one is z-polarized. This complicates the theoretical treatment predicting the reflection maxima according to the method of Decius, Frech and Bruesch (10). Nevertheless, by assuming appropriate polarization and crystal orientation the essential features can still be sorted out.

In addition to the strong reflection observed between the longitudinal and transverse absorption limits, Decius et al have demonstrated both experimentally and theoretically the existence of strong reflection from crystal faces at frequencies above the longitudinal mode. This reflection is observed at finite incidence angles from crystal faces normal to the transition dipole direction for vibrational modes. In the reference cited above this high frequency reflection band was explained theoretically for the uniaxial calcite crystal system. Using this method this author will extend their results to describe the reflection spectra observed for the orthorhombic K_2SO_4 crystal.

Consider the physical arrangement in which the radiation is taken at a finite angle from the xy face of K_2SO_4 with the plane of incidence being the xz plane. The z-polarized dipole is, therefore, perpendicular to the incident face with the x-polarized dipole parallel to the face and in the plane of incidence. This particular orientation is depicted in Figure 22.

The two types of polarization utilized in the experimental measurements were the TE and TM polarizations. In the TE mode the

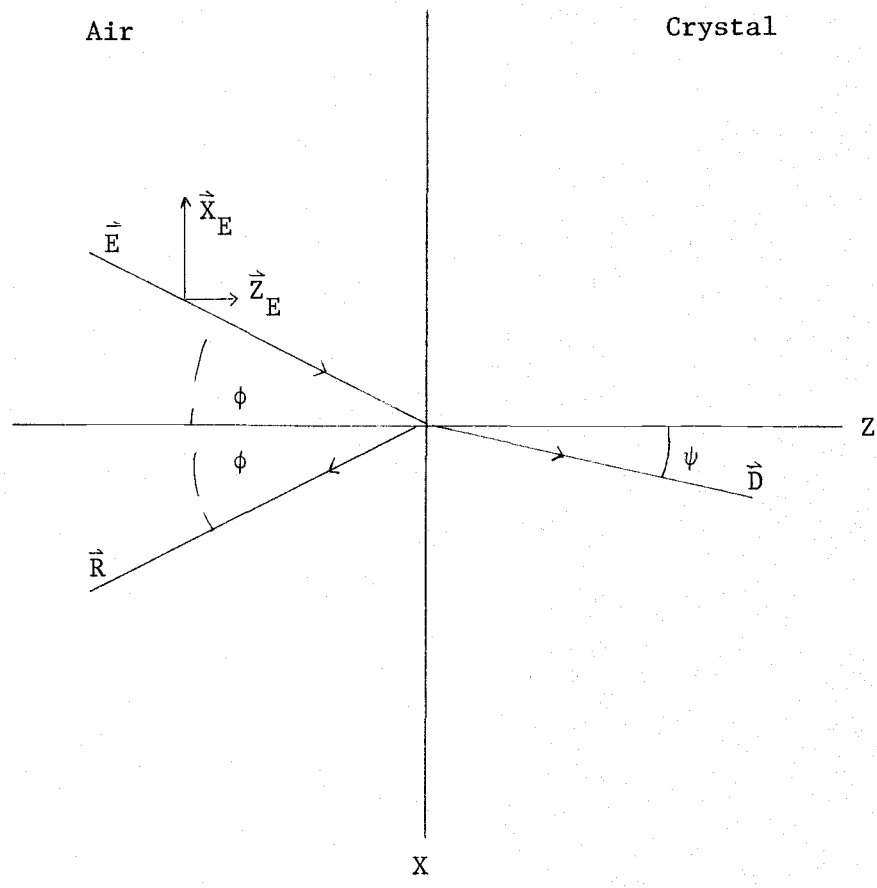

Figure 22. Schematic of Reflection Arrangement

incident radiation is polarized such that the resulting electric vector is perpendicular to the plane of incidence. The TE reflectivity will be independent of the angle of incidence, but there will be an angle dependence observed for the TM mode. In this case the electric vector of the polarized incident radiation lies in the plane of incidence. The latter case will be adopted in the following treatment.

From Fresnel's equation the complex dielectric constant of the transmitted wave propagating in a direction parallel to the xz plane and making an angle ψ relative to the z axis is given by the following relation.

$$\frac{1}{\varepsilon} = \frac{\sin^2\psi}{\varepsilon_z} + \frac{\cos^2\psi}{\varepsilon_x} \tag{2}$$

Snell's law relates the angle of the incident wave, ϕ, to that of the diffracted wave, ψ, in the equation given below.

$$\varepsilon^{\frac{1}{2}} \sin\psi = \sin\phi \tag{3}$$

Using Snell's law to eliminate ψ from Equation 3 gives

$$\varepsilon = \varepsilon_x + \sin^2\phi - \frac{\varepsilon_x}{\varepsilon_z}\sin^2\phi \tag{4}$$

The dielectric constant can be described as having the following principal values

$$\varepsilon_\sigma = \varepsilon_\sigma^\circ + \sum_k \frac{S_k^{(\sigma)}\omega_k^2}{\omega_k^2-\omega^2} \qquad j = x, y \text{ or } z \tag{5}$$

where

$$S_k^{(\sigma)} \sim \left(\frac{\partial \mu_i}{\partial Q_k}\right)^2 \tag{6}$$

The damping term has been omitted from the expression in the denominator of Equation 5 for simplification of the algebra. This approximation can be done without destroying the essential features of the phenomenon.

The dipole derivatives along the x-axis are well separated with respect to frequency so that the x component of the dielectric constant in the vicinity of ν_3 or ν_4 can be written as follows

$$\varepsilon_x \simeq \varepsilon_x^0 + \frac{S_k(x)\omega_k}{\omega_k^2 - \omega^2} \tag{7}$$

where

$$\varepsilon_x^0 = \varepsilon_x(\infty) + \sum_j \frac{S_j^{(x)}\omega_j^2}{\omega_j^2 - \omega_k^2} \tag{8}$$

Letting ω_{kL} represent the longitudinal frequency for this mode and noting that the dielectric constant passes through zero at this value gives

$$S_k^{(x)}\omega_k^2 = \varepsilon_x^0(\omega_{kL}^2 - \omega_k^2) \tag{9}$$

Substituting this relation into Equation (7) and collecting terms gives

$$\varepsilon_x = \varepsilon_x^0 \frac{(\omega_{kL}^2 - \omega^2)}{(\omega_k^2 - \omega^2)} \tag{10}$$

Similarly, Equation 5 can be used to derive an expression for the z component of the dielectric constant in Equation 4. This case is somewhat more complicated than the previous one since there are two components of z polarization in each of the spectral regions ν_3 and ν_4. Since the spectral regions are well separated only two components need to be considered at one time. In this case Equation 5 becomes

$$\varepsilon_z \simeq \varepsilon_z^o + \frac{S^{(z)}_{k_1}\omega^2_{k_1}}{(\omega^2_{k_1} - \omega^2)} + \frac{S^{(z)}_{k_2}\omega^2_{k_2}}{(\omega^2_{k_2} - \omega^2)} \qquad (11)$$

Again the longitudinal frequencies associated with the two components are defined to be $\omega_{k_1L} \rightarrow \omega_{k_2L}$, respectively. Since the real part of the dielectric constant is zero at the longitudinal frequencies the resulting two equations can be solved simultaneously for $S^{(z)}_{k_1}\omega_{k_1}$ and $S^{(z)}_{k_2}\omega_{k_2}$.

$$\varepsilon_z^o + \frac{S^{(z)}_{k_1}\omega^2_{k_1}}{(\omega^2_{k_1} - \omega^2_{k_1L})} + \frac{S^{(z)}_{k_2}\omega^2_{k_2}}{(\omega^2_{k_2} - \omega^2_{k_1L})} = 0 \qquad (12)$$

and

$$\varepsilon_z^o + \frac{S^{(z)}_{k_1}\omega^2_{k_1}}{(\omega^2_{k_1} - \omega^2_{k_2L}} + \frac{S^{(z)}_{k_2}\omega^2_{k_2}}{(\omega^2_{k_2} - \omega^2_{k_2L})} = 0 \qquad (13)$$

Substituting these solutions back into Equation (11) gives

$$\varepsilon_z = \varepsilon_z^o + \frac{\varepsilon_z^o(\omega^2_{k_1L} - \omega^2_{k_1})}{(\omega^2_{k_2} - \omega^2_{k_1} - \omega^2)} + \varepsilon_z^o \frac{(\omega^2_{k_2L} - \omega^2_{k_2})(\omega^2_{k_2} - \omega^2_{k_1L})}{(\omega^2_{k_2} - \omega^2_{k_1})(\omega^2_{k_2} - \omega^2)}$$

and upon rearrangement

$$\varepsilon_z = \varepsilon_z^o \frac{(\omega^2_{k_{1_L}} - \omega^2)(\omega^2_{k_{2L}} - \omega^2)}{(\omega^2_{k_1} - \omega^2)(\omega^2_{k_2} - \omega^2)} \tag{15}$$

It is interesting to note that while the above equation resulted from the consideration of two components in the same frequency range the form of the equation finally reduces to a product of terms identical in form to the term derived in Equation 10 in which only one component is considered. This leads to the speculation that the following relation may in general be true although no proof is attempted here.

$$\varepsilon_\sigma = \varepsilon_\sigma^o + \sum_k \frac{S^\sigma{}_k \omega^2_k}{\omega^2_k - \omega^2} \tag{16}$$

implies

$$\varepsilon_\sigma = \varepsilon^o{}_\sigma \prod_k \frac{(\omega^2_{kL} - \omega^2)}{(\omega^2_k - \omega^2)} \tag{17}$$

The expressions for the x and z components of the dielectric constant given in Equations 10 and 15 are then substituted into Equation 4 yielding

$$\varepsilon(\omega,\phi) = \frac{\varepsilon_x^o (\omega^2_{kL} - \omega^2)}{(\omega^2_k - \omega^2)} + \mathrm{Sin}^2\phi - \frac{\varepsilon_x^o}{\varepsilon_z^o} \frac{(\omega^2_{kL} - \omega^2)(\omega^2_{k_1} - \omega^2)(\omega^2_{k_2} - \omega^2)}{(\omega^2_k - \omega^2)(\omega^2_{k_{1L}} - \omega^2)(\omega^2_{k_{2L}} - \omega^2)} \mathrm{Sin}^2\phi \tag{18}$$

where $\varepsilon_x^o = \varepsilon_x^o(\infty) + \sum_{j \neq k} \frac{S^{(x)}_j \omega^2_j}{(\omega^2_j - \omega^2_k)}$

ω_k = the frequency of the transmission minimum for mode k which is x-polarized.

ω_{kL} = the longitudinal frequency for mode k.

ϕ = the angle that the incident radiation makes with respect to the normal to the crystal face.

$$\varepsilon^{o}_{z} = \varepsilon_{z}(\infty) + \sum_{j \neq k} \frac{S^{(z)}_{j} \omega^{2}_{j}}{(\omega^{2}_{j} - \omega^{2}_{k_1})} + \sum_{j \neq k_2} \frac{S^{(z)}_{j} \omega^{2}_{j}}{(\omega^{2} - \omega^{2}_{k_2})}$$

ω_{k_1} = the frequency of the transmission minimum for mode k_1 which is z-polarized.

$\omega_{k_1 L}$ = the longitudinal frequency for mode k_1.

ω_{k_2} = the frequency of the transmission minimum for mode k_2 which is z-polarized.

$\omega_{k_2 L}$ = the longitudinal frequency for mode k_2.

The above equation gives the frequency and angle dependence of the dielectric constant for that crystal orientation shown in Figure 22 and in the vicinity of either ν_3 or ν_4 of the orthorhombic K_2SO_4 system.

Equation 18 predicts correctly that at normal incident reflection, that is when $\phi = 0$, only the x component attributes to the reflectivity with a band between ω_k and ω_{kL}. At finite angles of incidence poles are indicated at $\omega = \omega_k$, ω_{k1L} and ω_{k2L}.

This expression is very similar to that derived by Decius et al (10) for the simpler uniaxial crystal system in which they further simplified the mathematics by considering that particular crystal orientation isolating one absorbing mode as compared to the three components treated here. As a result they were able to show the existence of a zero in their expression for the dielectric constant at a frequency ω_{kLL} above ω_{kL} thus predicting correctly the reflectivity

spectra showing bands above the longitudinal frequency under certain crystal arrangements.

Due to the complexity of Equation 18 no such solutions were obtained. Setting $\varepsilon(\omega,\phi) = 0$ and solving for the corresponding values of ω does yield an equation cubic in ω^2 which theoretically does have solutions. However, derivation of these solutions is beyond the scope of this work.

Drawing upon the similarities between the two equations and the experimental spectra obtained in this work some of which show high frequency bands associated with the normal reflection bands it can be speculated that solutions to the above mentioned cubic equation would also predict values above the longitudinal frequencies.

The experimental spectra in the vicinity of the sulfate mode obtained from reflection measurements at incident angles of 38^{o} and 52.5^{o} are presented in Figure 23. The crystal was oriented to correspond to the arrangement used in the preceding theoretical discussion. The band above 1175 cm^{-1} is at a higher frequency than observed for any of the near-normal spectra and is believed to correspond to a high frequency component of the z-polarized mode, ω_{k_2}. The intensity of this band appears to show a dependence on the indicent angle with the greater peak height occurring at the larger angle.

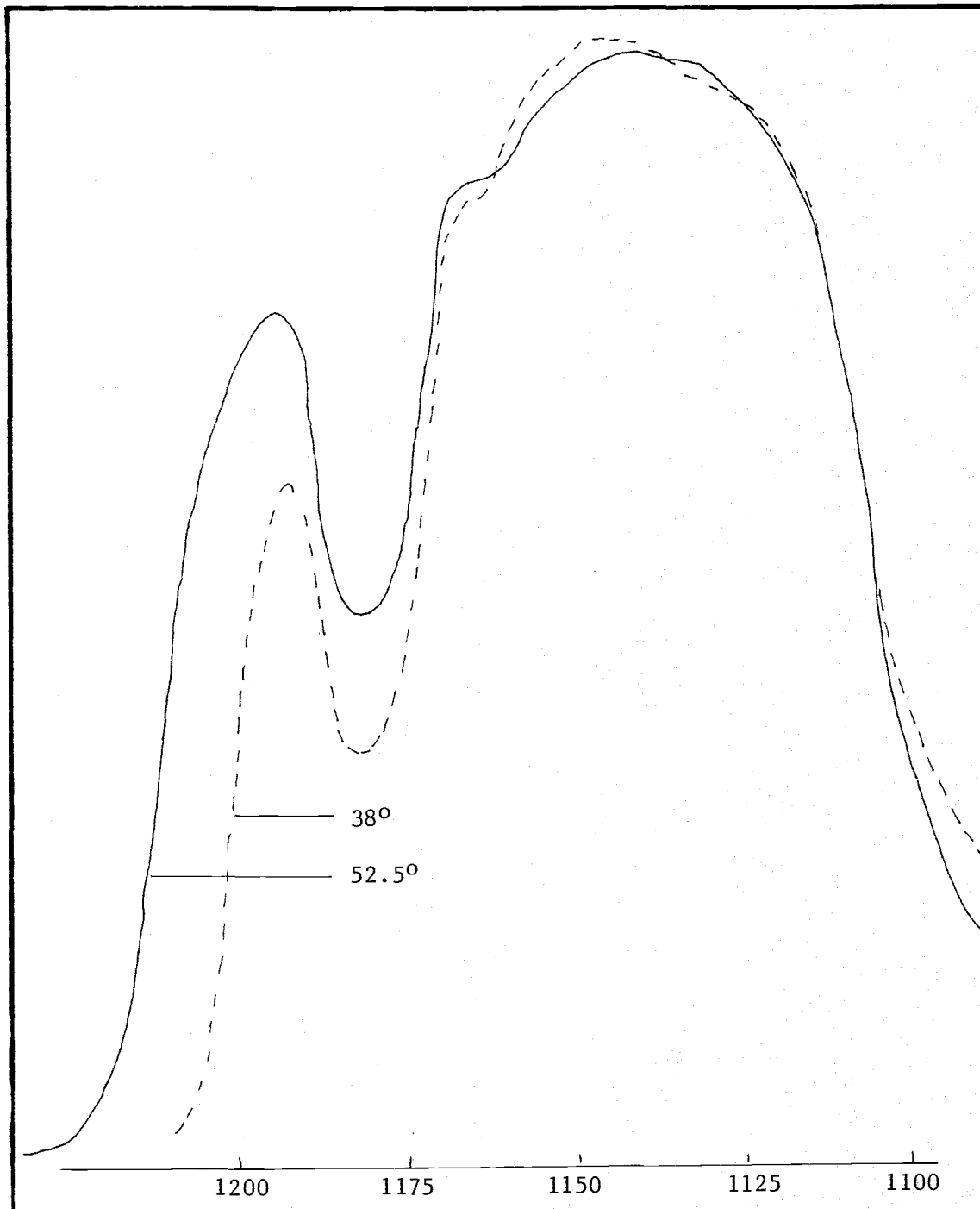

Figure 23. Reflection Spectra showing the angle dependence of the high frequency band in the TM mode for the sulfate ν_3 absorption

VI. INFRARED TRANSMISSION SPECTRA OF K_2SO_4

Thin sections of K_2SO_4 crystals were prepared according to the procedure described in a previous section. Two distinct orientations of the crystalline sections were prepared, one of which was coplanar with the 010 plane and the other coplanar with the 001 plane. The x-polarized spectra were obtained by scanning the transmission produced when the resultant $\vec{E}_m$ of the linearly polarized radiation was aligned parallel to the a axes of the crystals as shown in the following diagram.

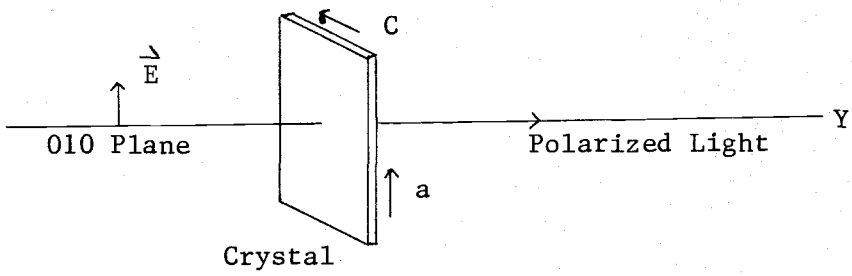

Correspondingly, the y-polarized spectra were obtained by aligning the b axes of the crystals cut coplanar to the 001 plane parallel to the electric vector of the incident radiation and the z-polarized spectra by aligning the c axes of the crystals cut coplanar to the 010 plane parallel to the electric vector. The x-polarized spectra

could also be obtained from the 001 sections with proper orientation, thus providing a check on the relative thicknesses and orientation of two sections representing the two different planes.

Due to the small cross-sectional areas of the samples, it was necessary to mount them in a beam condenser to obtain sufficient energy in the spectrometer. For this reason the light incident on the crystal was not entirely normal. No attempt, however, will be made to interpret this effect on the resulting spectra. The sample holder used with the beam condenser could be rotated so that the two orientations of a particular crystal section with respect to the polarized light were produced by rotating the sample as opposed to rotating the polarizer. Rotation of the polarizer was limited by the severe loss of energy caused by cross-polarization produced between the polarizer and the optics of the instrument at certain polarizer positions. Therefore, in practice the polarizer was adjusted to obtain minimum cross-polarization and the crystal was then aligned with the resulting electric vector.

A. Fundamental Vibrational Spectra

The transmission spectra of the fundamental sulfate vibrational regions of thin crystalline sections of K_2SO_4 provided limited information as to the exact position of the maximum absorbance of the bands. The thinnest crystal section obtained was approximately 4-5μ thick, however, the absorption bands due to ν_3 and ν_4 vibrational modes were still very broad and unresolved.

A free sulfate ion exhibiting tetrahedral symmetry has four fundamental vibrational transitions. The totally symmetric mode, ν_1, (981 cm^{-1}) is a non-degenerate vibration of the symmetry species A_1. It is a Raman allowed and infrared forbidden mode as long as the ion retains its tetrahedral symmetry. The sulfate ion in the K_2SO_4 lattice exhibits less than tetrahedral symmetry since its site symmetry is C_s. As shown in section 4.1 the application of the correlation diagram for this situation predicts that ν_1 will be infrared active, capable of coupling with y- and z-polarized radiation, but not x-polarized. From Figures 24, 25, and 26 it can be seen that in the y- and z-polarized spectra a band is observed at 983 cm^{-1} but is missing in the x-polarized spectrum just as predicted. The spectra shown in dashed lines were obtained using a crystal approximately 4-5μ thick. It was prepared parallel to the 021 face. This plane in conjunction with the polarized radiation permitted a pure x polarization arrangement and by rotating the crystal 90^{o} a yz polarization was obtained. The ν_1 band obtained from the yz polarization has a minimum of 983 cm^{-1} which corresponds very closely to the Raman value of 984 cm^{-1}.

The doubly degenerate mode ν_2 occurs near 451 cm^{-1}. The spectra in Figures 24, 25 and 26 show a doublet in each case. The low frequency band is believed to be caused by the instrumental arrangement and not the crystal. The three components obtained under the three polarizations display a directional dependence for the intensity as well as the position of the absorptions.

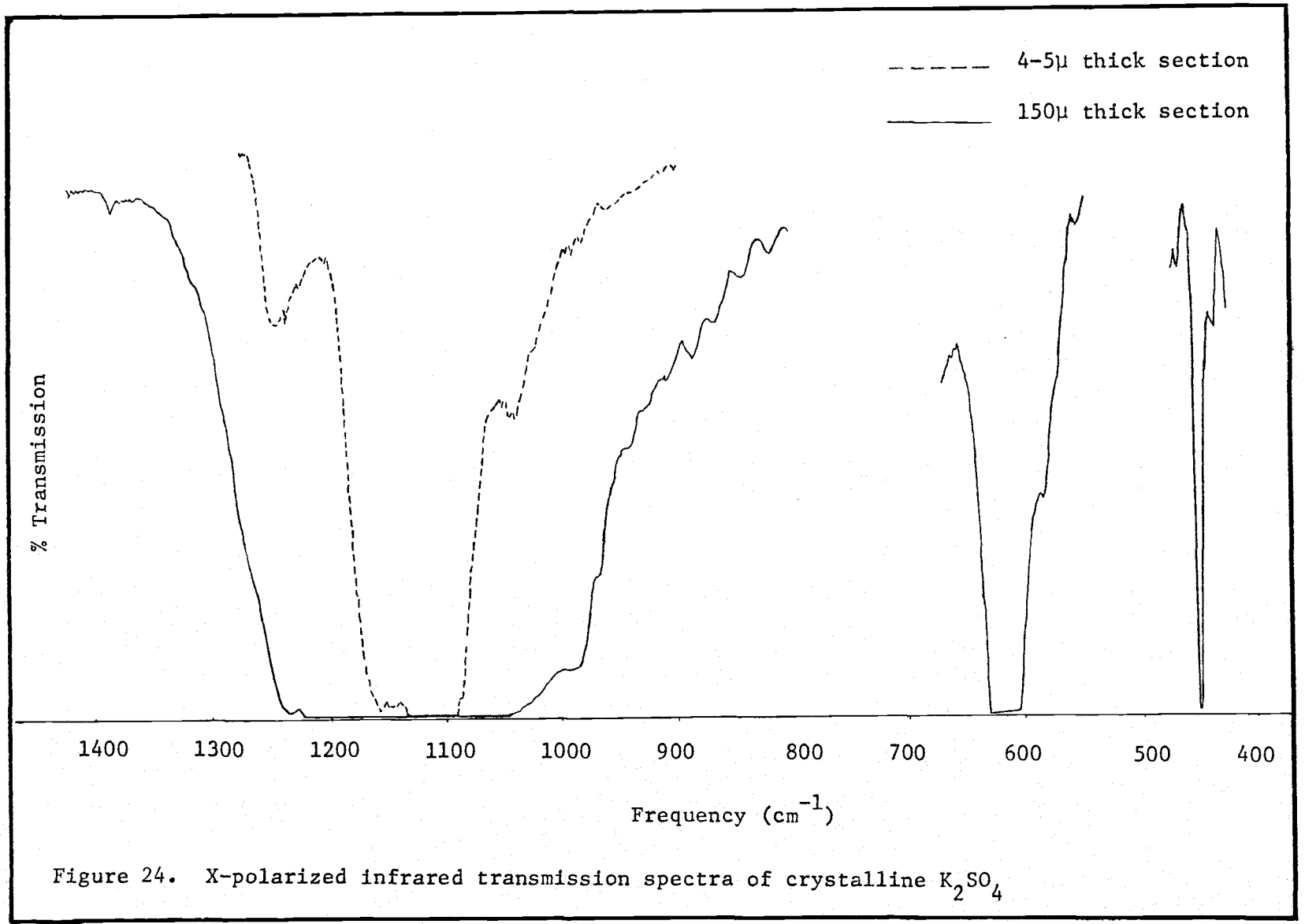

Figure 24. X-polarized infrared transmission spectra of crystalline K_2SO_4

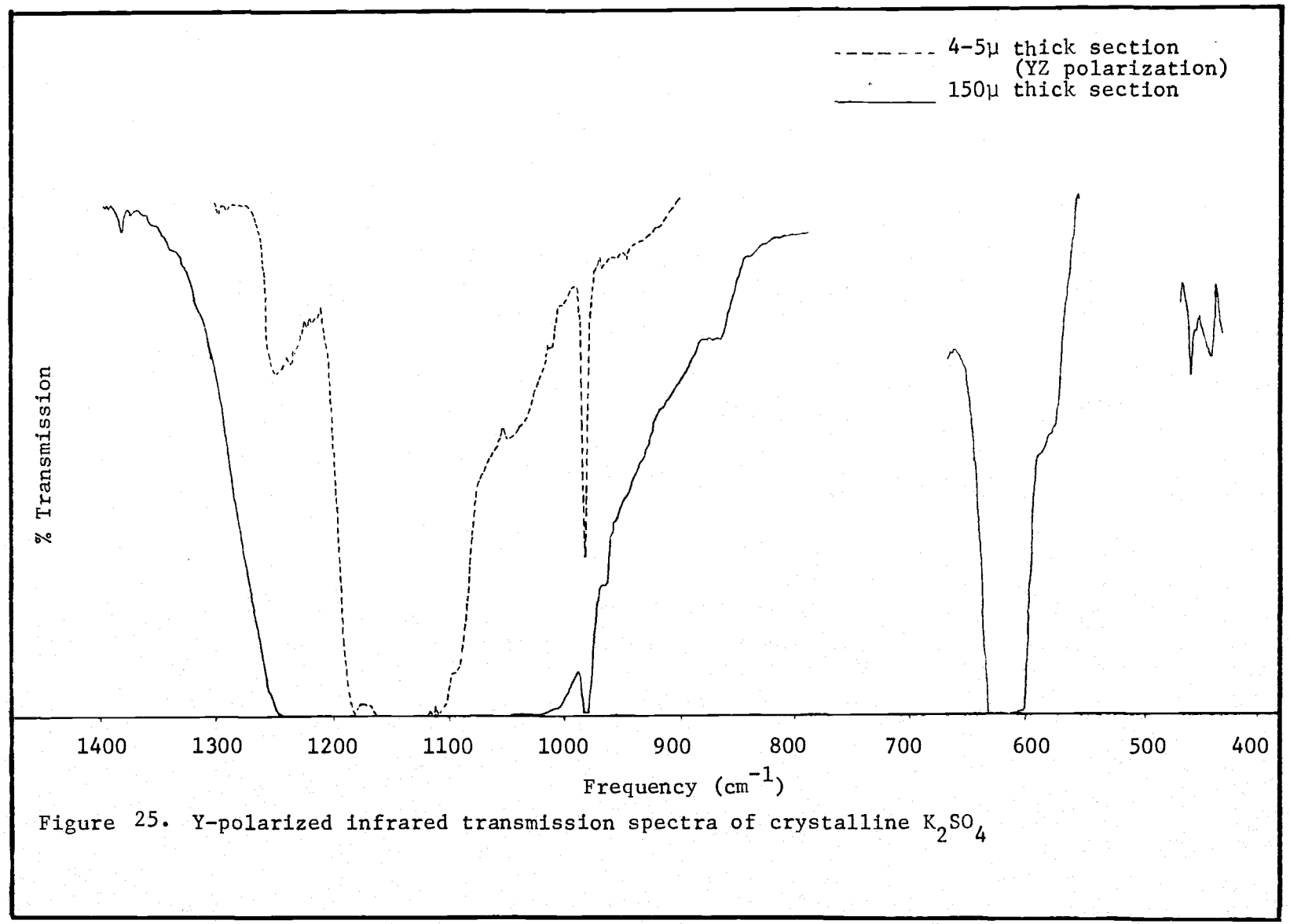

Figure 25. Y-polarized infrared transmission spectra of crystalline K_2SO_4

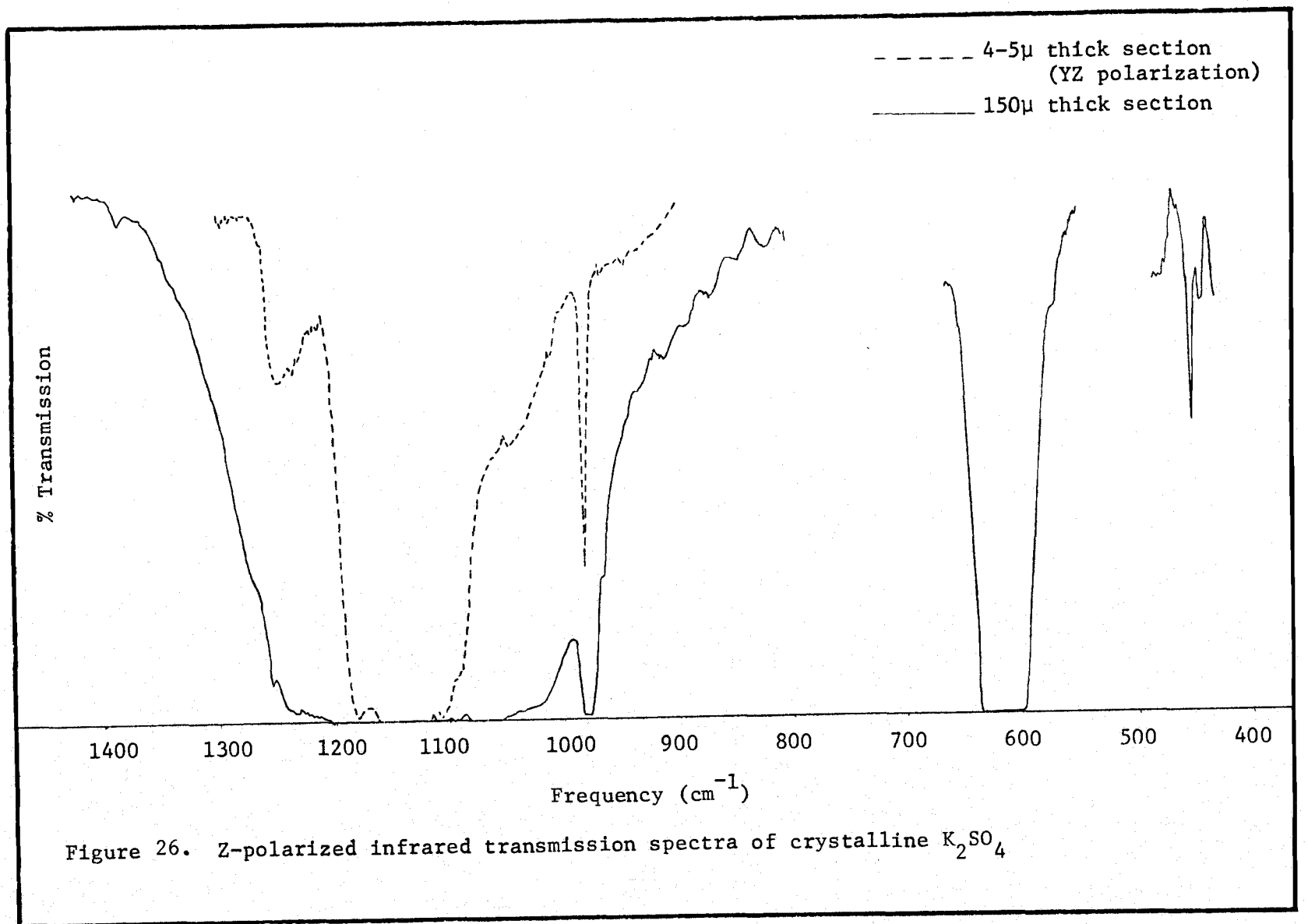

Figure 26. Z-polarized infrared transmission spectra of crystalline K_2SO_4

The triply degenerate modes ν_3 and ν_4 occur near 613 and 1104 cm^{-1} (1), respectively. These two absorptions are so intense (see Figures 24, 25 and 26) that even at crystal thicknesses of a few microns the transmission is zero near the maximum absorbance. For this reason very little information can be gained directly from the transmission spectra in these two regions.

B. Overtone and Combinational Spectra

The transmission spectra obtained between 1300-4000 cm^{-1} from thin sections of K_2SO_4 revealed many distinct bands. Spectra taken under polarization show that the absorptions are different depending on the orientation of the sample to the electric vector. These bands are believed to arise from combinations and overtones of the fundamental absorptions. Even though there are quite a number of peaks appearing this is a relatively small number compared to the number of combinations and overtones allowed by symmetry. It seems that there is quite a selective rule governing the intensity of an overtone or combination band. In other words it may be that even though a combination or overtone transition is allowed by summetry it is of such low intensity that it is not observed in the sections examined.

1. 1500-1700 cm^{-1}

The bands observed in the region from 1500-1700 cm^{-1} consist mainly of a pair of incompletely resolved bands. The x-polarized spectrum shows two bands fairly free of side structure while in the y- and z- polarization more structure appears to be associated with the prominent bands as seen in Figure 27. The structure at approximately 1550 cm^{-1} is assigned to the combination $\nu_2 + \nu_3$. Using the selection rules for overtones and combinations shown in Table 9, an attempt has been made to assign the observed spectra in a logical and consistent manner. This is quite difficult since by the factor group analysis selection rules some bands can be accounted for quite accurately by several choices whereas, as will be seen later, some bands appear to have no good assignment. The factor group analysis was chosen over the simpler site group analysis because the former allows more selectivity in the choice of overtones and combinations of the fundamentals allowed, however, as pointed out previously, not even this appears to be stringent enough as demonstrated by the observed spectra.

The spectra in this region were obtained from thin sections of approximately 200μ thick and of two orientations, namely sections coplanar to the 010 and 001 planes.

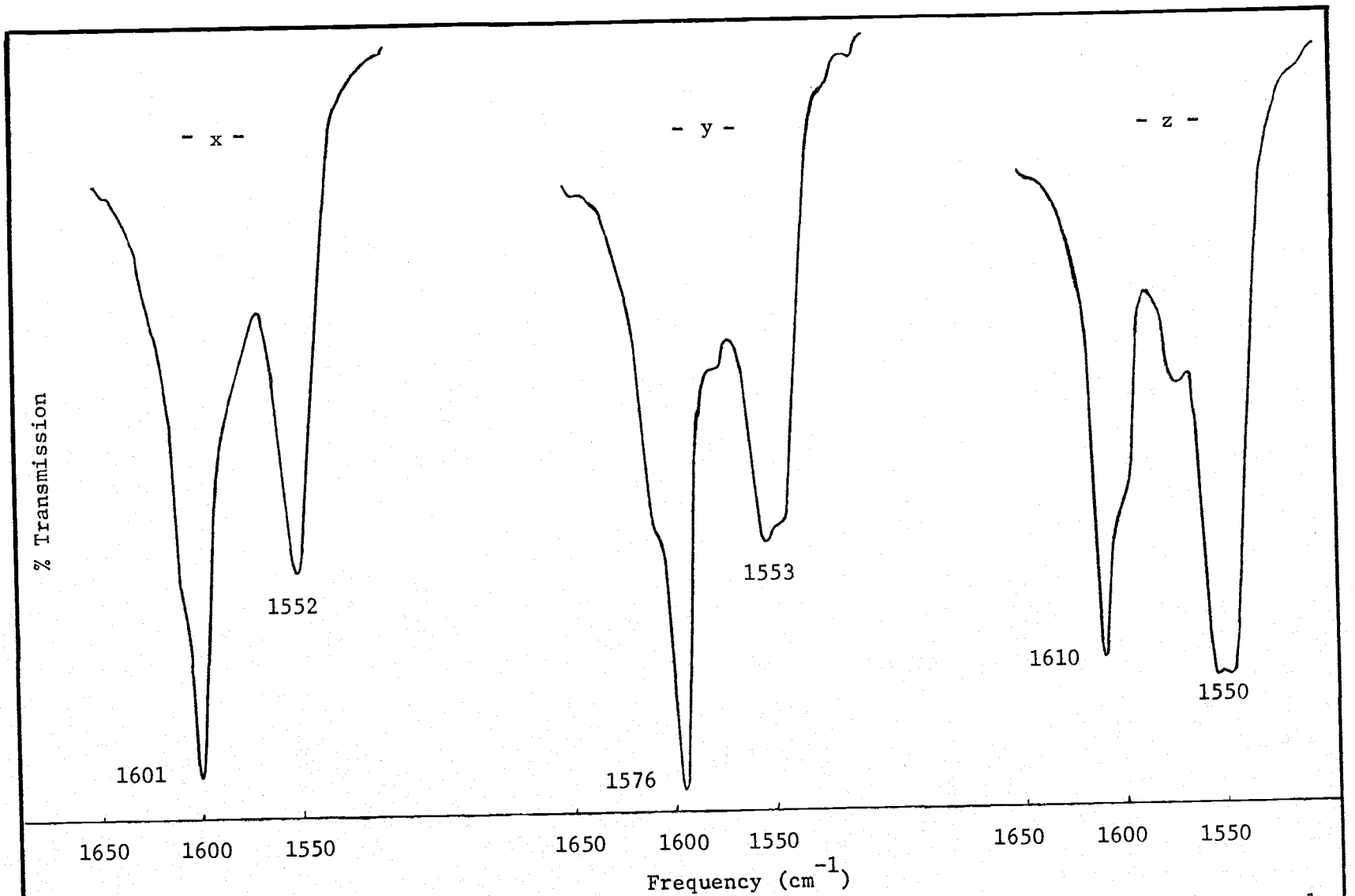

Figure 27. The combination region of $\nu_2+\nu_3$ and $\nu_1+\nu_4$ under X,Y,and Z polarization of K_2SO_4 crystals approximately 200μ thick

Table 9. Combination and Overtone Frequencies for Crystalline K_2SO_4

Combination or Overtone Frequencies	Observed Polarization	Possible Assignment
1547 (sh)	Z	
1548 (sh)	Y	
1552	X	$\nu_2+\nu_3$
1553	Y	
1554	Z	
1596	Y	
1601	X	
1610	Z	
1720	X	$\nu_1+\nu_4$
1722	Y	
1724	Z	
1743 (sh)	Y	$\nu_3+\nu_4$
1785	X	
1787	Y	
1788	Z	
1965	Y, Z	$2\nu_1$
2074	Y	
2082	X	
2104 (sh)	Y	$\nu_1+\nu_3$
2116 (sh)	Z	
2130	Z	
2143	Y	
2144	X	
2204	X	
2206	Y, Z	
2226 (sh)	X, Y	
2262 (sh)	Y	
2265	X, Z	$2\nu_3$
2278	Y	
2295 (sh)	Y	
2295	Z	
2316 (sh)	Z	

2. 1700-1800 cm^{-1}

In order to attain sufficient intensity (to observe the structure) in the absorptions in this region, section thicknesses of approximately 700μ were necessary. Again, two main bands were observed separated by about 65 cm^{-1}. This compares to a separation of approximately 50 cm^{-1} in the previously discussed bands. The position of the maximum absorbances remained fairly consistant among the three polarizations, while the relative intensities varied in each case. As seen in Figure 28 and the bands are relatively narrow with some side structure in the y- and z-polarized spectra. This region is assigned to the combination, $\nu_3 + \nu_4$, although the bands at 1785-1787 cm^{-1} must be assigned negative anharmonicity to get a value that high using the observed values of the fundamentals.

3. 1950-2000 cm^{-1}

The spectra taken in this region were also made from 700μ thick samples. This region corresponds to that of the first overtone of fundamental ν_1. As predicted by theory, either the site or factor group analysis, no absorption is observed in the x-polarized spectrum as shown in Figure 29. Bands at 1965 cm^{-1} are found in the spectra of both the y- and z- polarized arrangements. The relative intensities of the two bands agree, at least qualitatively, with the

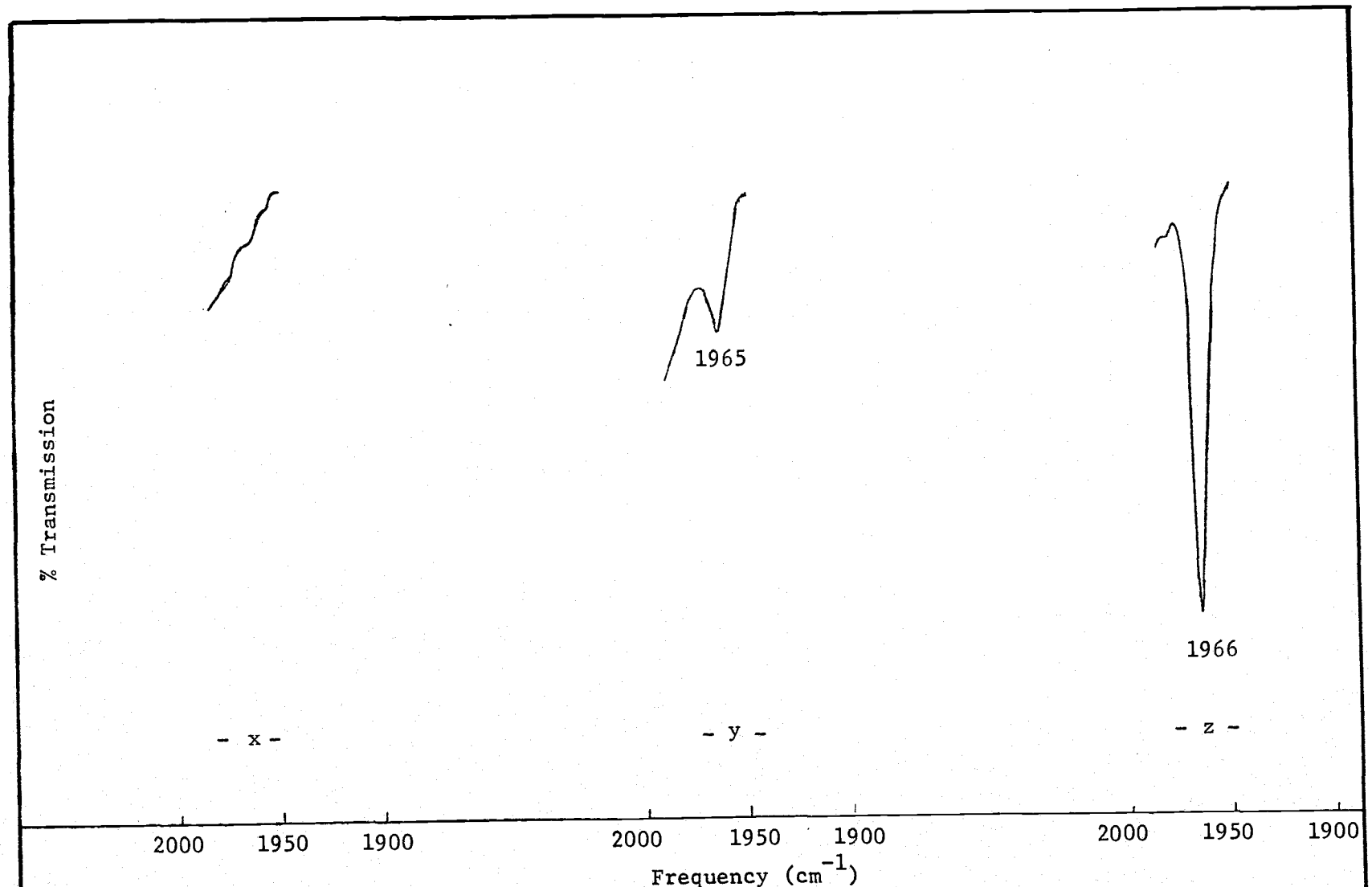

Figure 28. The overtone region of ν_1 under x, y and z polarization of K_2SO_4 crystals approximately 700μ thick

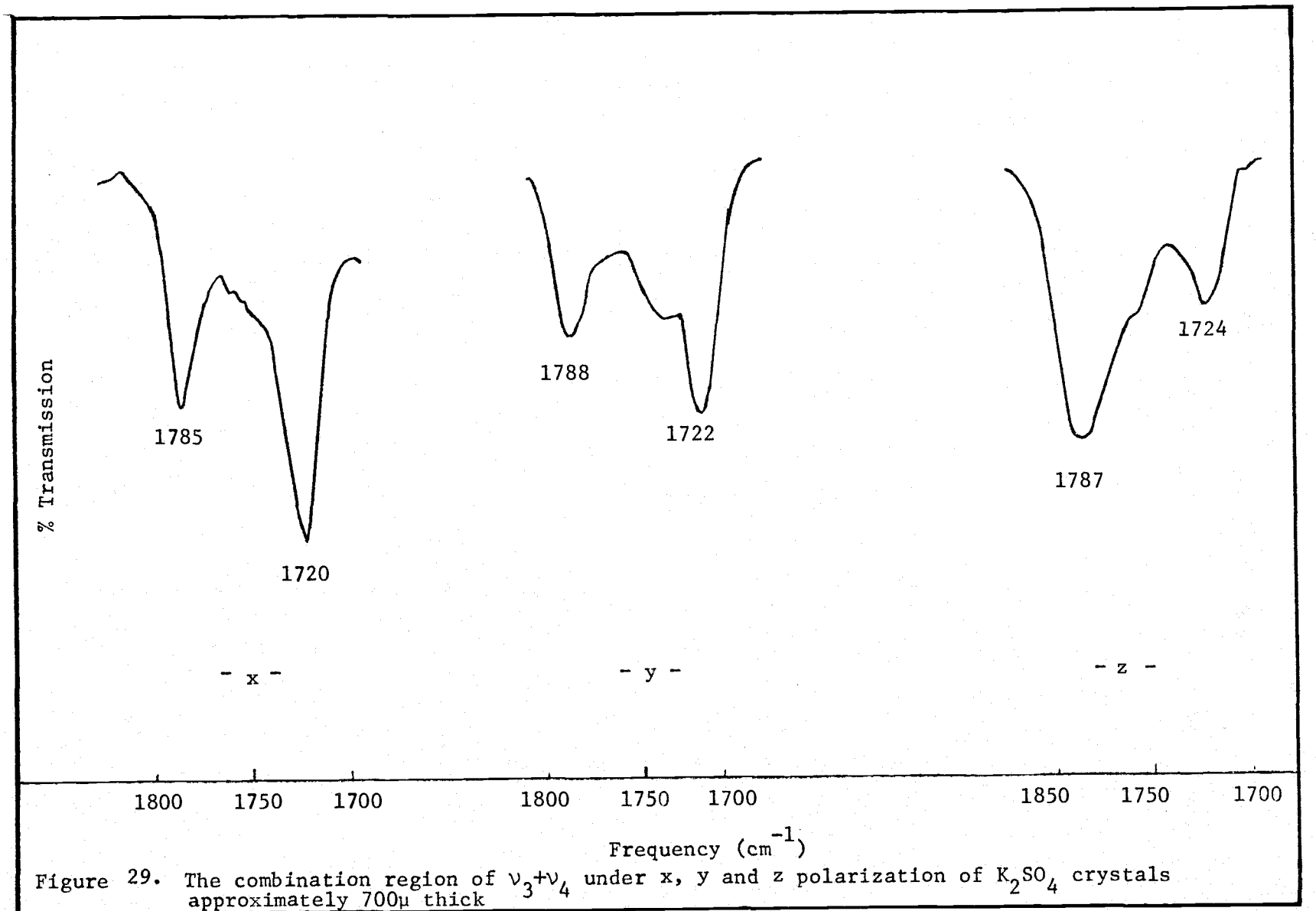

Figure 29. The combination region of $\nu_3+\nu_4$ under x, y and z polarization of K_2SO_4 crystals approximately 700μ thick

observed intensity of the infrared active components in Figure 24. Although these bands are referred to as overtones, they are more correctly thought of as combinations of the 984 cm^{-1} (A_g) Raman active mode with 983 cm^{-1} (B_{1u} and B_{2u}) I. R. active modes.

4. 2000-2200 cm^{-1}

The spectra shown in Figure 30 were obtained from 150μ thick sections and the absorptions in this region were the most intense of the overtone and combination structure. This region is assigned to the combination, $\nu_1 + \nu_3$, but the two features at 2144 and 2143 cm^{-1} in the x- and y-polarizations, respectively, do not seem to be accounted for from the observed components of the fundamentals. The author feels that a correct assignment of the combinations that lead to these bands will provide the key to unravelling the total assignment pattern. There is always the possibility that symmetry species Au according to the factor group approach which is neither I.R. nor Raman active may enter into combination with other fundamentals thus explaining some of the bands observed.

The structure in the x- and y-polarized spectra in this region are quite similar qualitatively and quantitatively. The z-polarized spectrum, on the other hand is quite different. Instead of two main bands of approximately 2080 and 2140 cm^{-1} as in the x- and y-polarized case, there is one strong feature which appears to be made up of at least two incompletely resolved bands occurring between

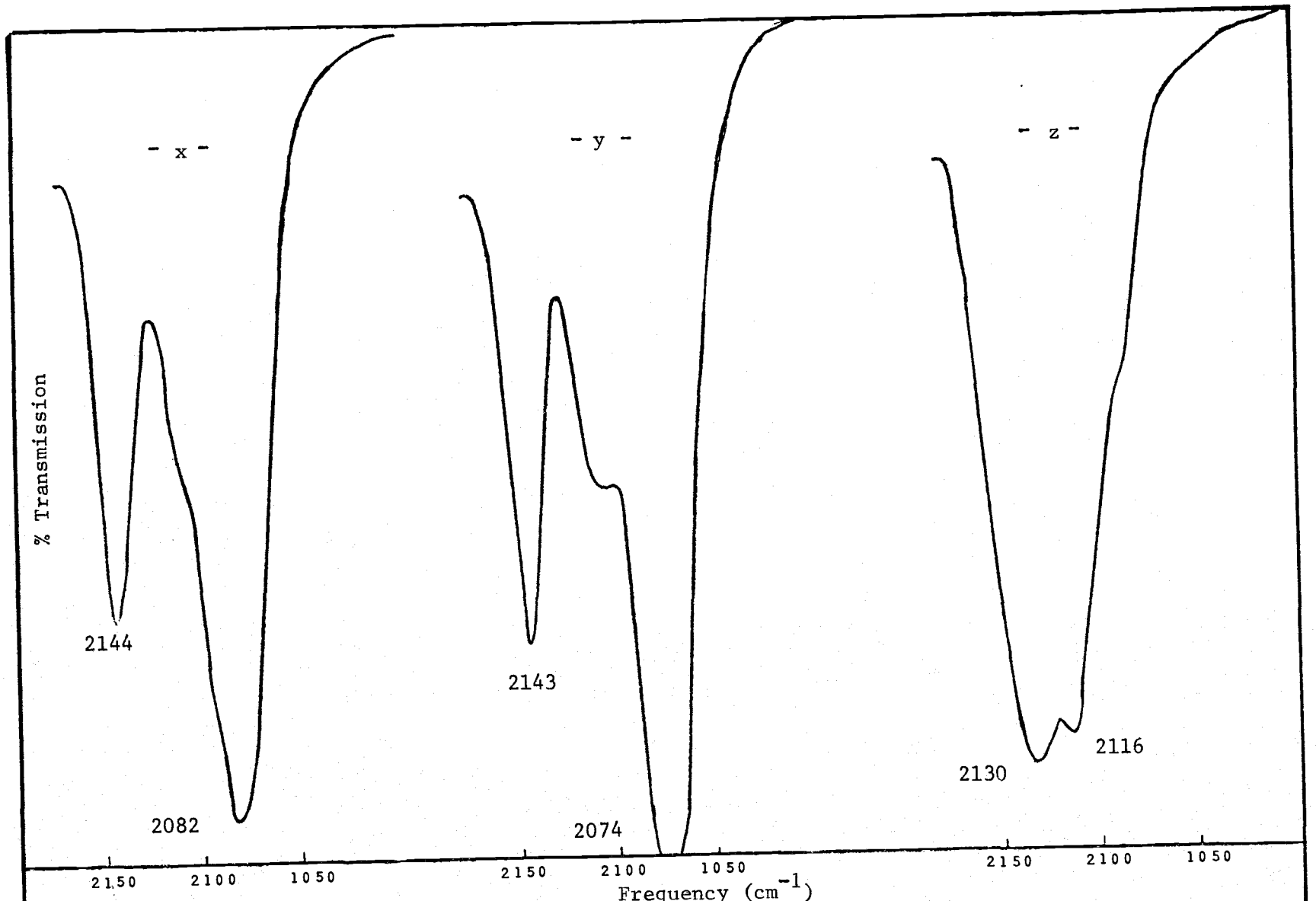

Figure 30. The combination of $\nu_1+\nu_2$ under x, y and z polarization of K_2SO_4 crystals approximately 150μ thick

the two bands mentioned above. As mentioned above, some interesting selection phenomena are demonstrated in this region.

5. 2200-2400 cm^{-1}

The final structure observed below 4000 cm^{-1} occurs between 2200 and 2400 cm^{-1}. Structure in this region is attributed to the first overtone of ν_3. Figure 31 shows the greatest variations observed among the three polarizations.

6. General comments concerning the overtone and combination regions

Although the precise selection rules governing the structure of the overtone and combination regions could not be ascertained, these spectra are presented in the hopes that in combination with spectra obtained in the study of related crystal systems a unique solution may be found. Since it appears that very little information can be obtained from the fundamental absorption regions by transmission studies, the overtone and combination spectra are a potential source of information leading to a description of the absorption phenomena in crystals.

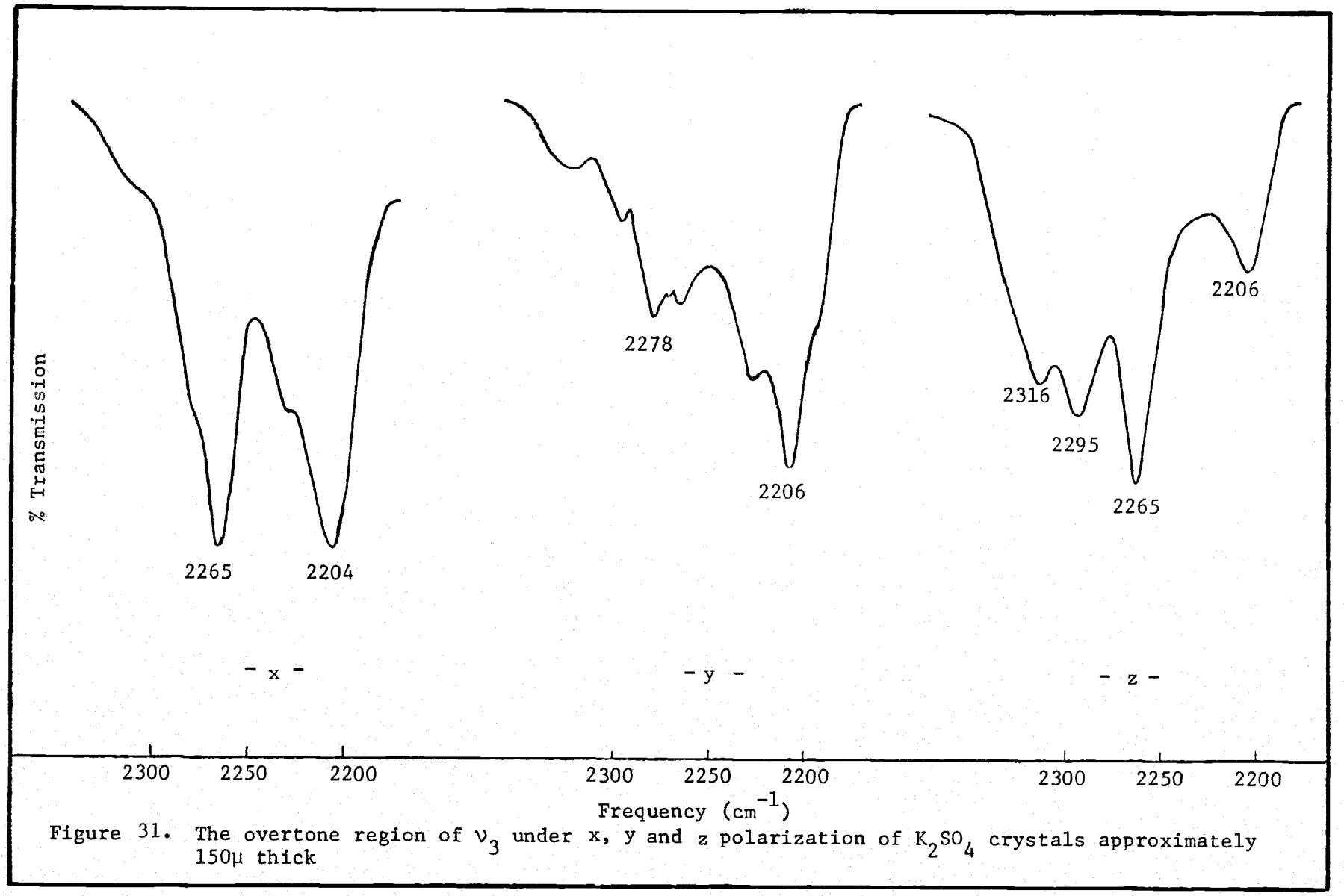

Figure 31. The overtone region of ν_3 under x, y and z polarization of K_2SO_4 crystals approximately 150μ thick

VII. COMPARISON OF SPECTRA FROM THE ABOVE THREE TECHNIQUES

Although neither infrared transmission, infrared reflection nor Raman spectroscopy can give all of the information necessary to assign all of the symmetry species allowed under a factor group analysis, the combination of all three provide a fairly complete set of data. Although the transmission spectra give little more than the general region of the fundamental absorptions for ν_3 and ν_4 it is interesting to compare intensities and band widths with the reflection spectra. Figures 32, 33 and 34 compare the three types of spectra taken under similar polarization arrangements. The transmission and reflection spectra for a given polarization each have the electric vector in the same direction. The Raman spectra are categorized according to the diagonal term of the polarization tensor being determined, for instance the Raman spectra of the polarization tensor, α_{xx}, is compared to the x polarization of the transmission and reflection spectra.

Table 10 lists the vibrational frequencies along with their assignments according to a factor group analysis. The frequencies are grouped into the four fundamental regions and are denoted as to which analytical technique was used to obtain them.

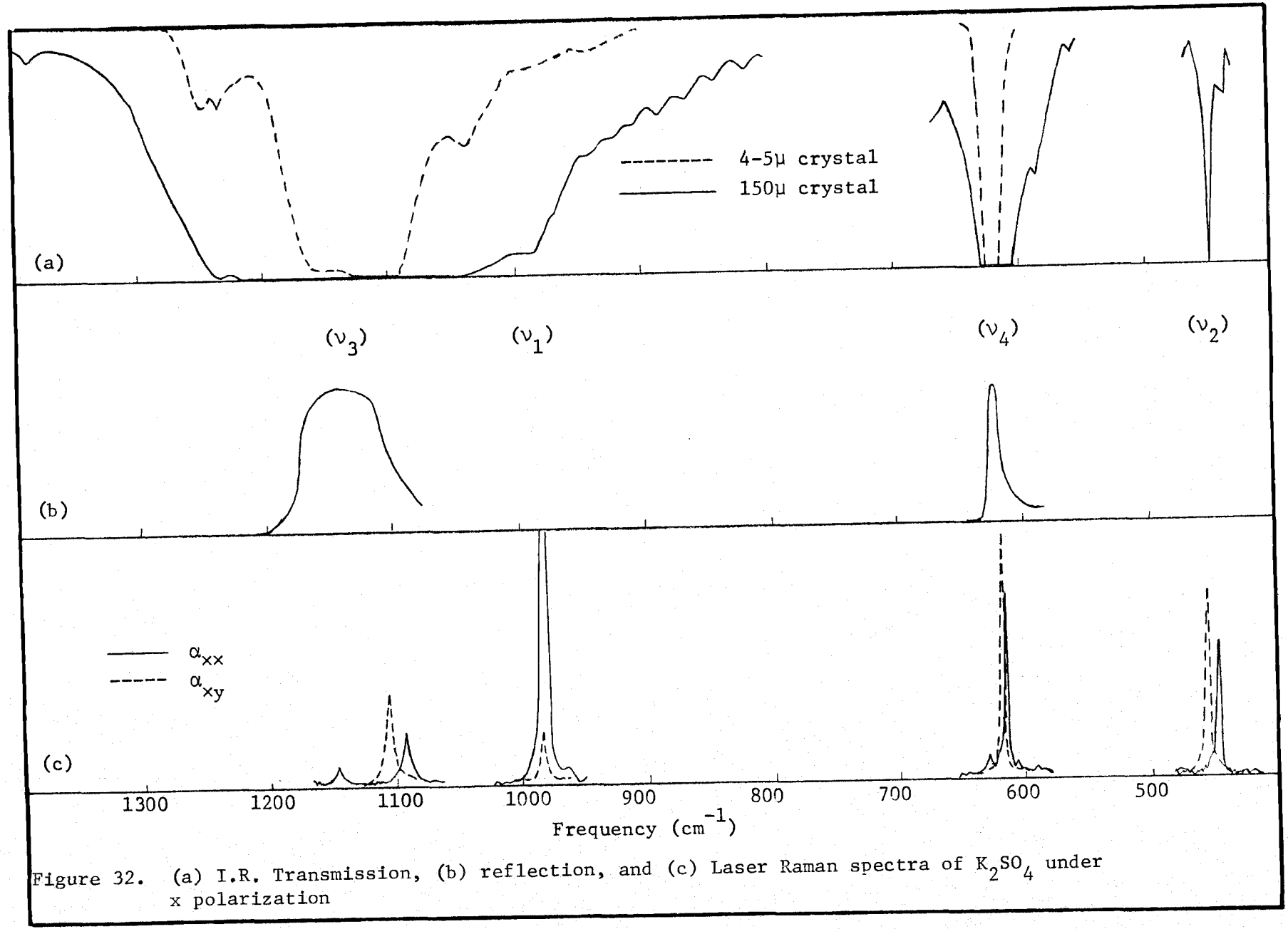

Figure 32. (a) I.R. Transmission, (b) reflection, and (c) Laser Raman spectra of K_2SO_4 under x polarization

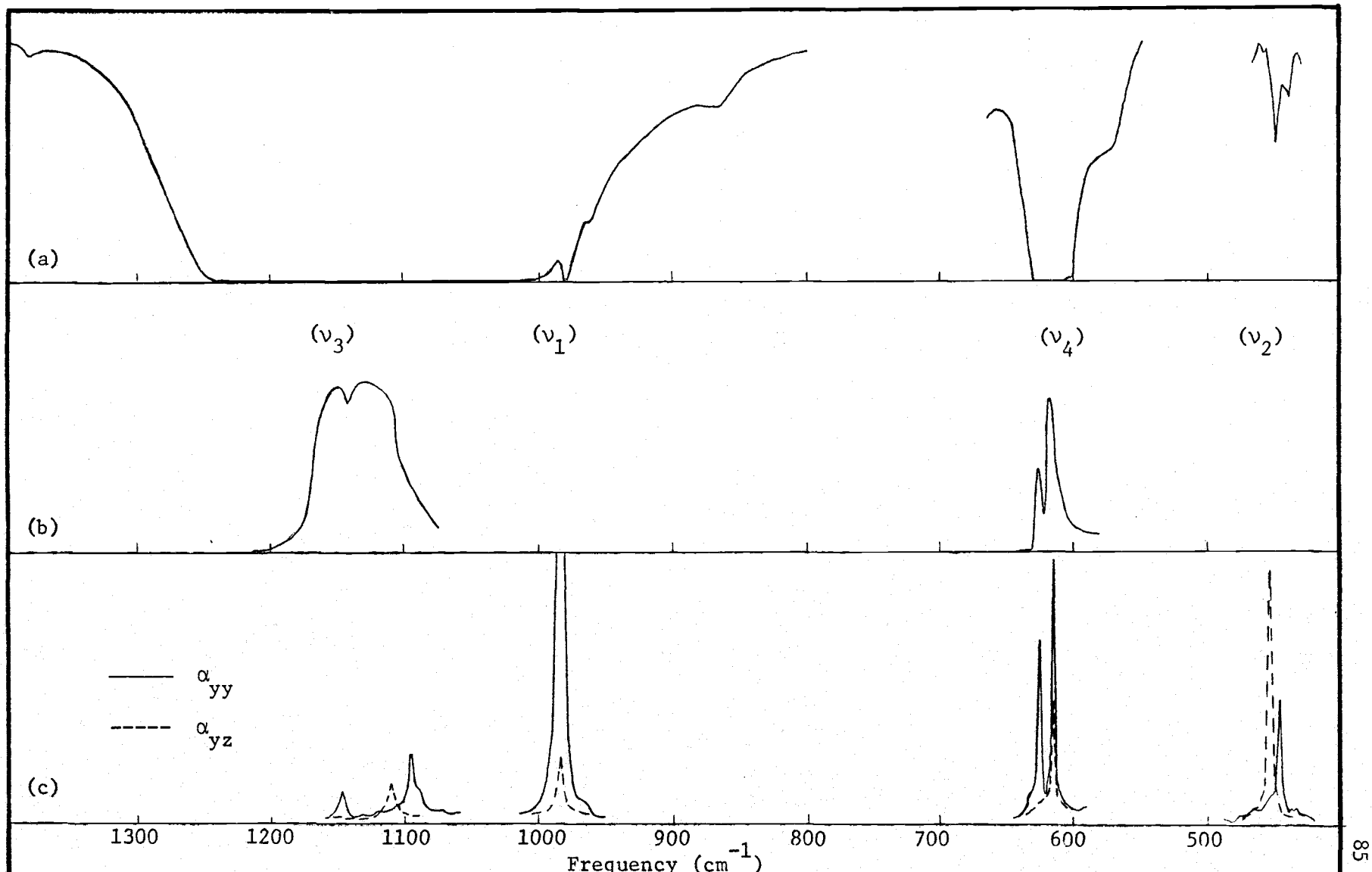

Figure 33. (a) I.R. Transmission, (b) reflection, and (c) Laser Raman spectra of K_2SO_4 under y polarization

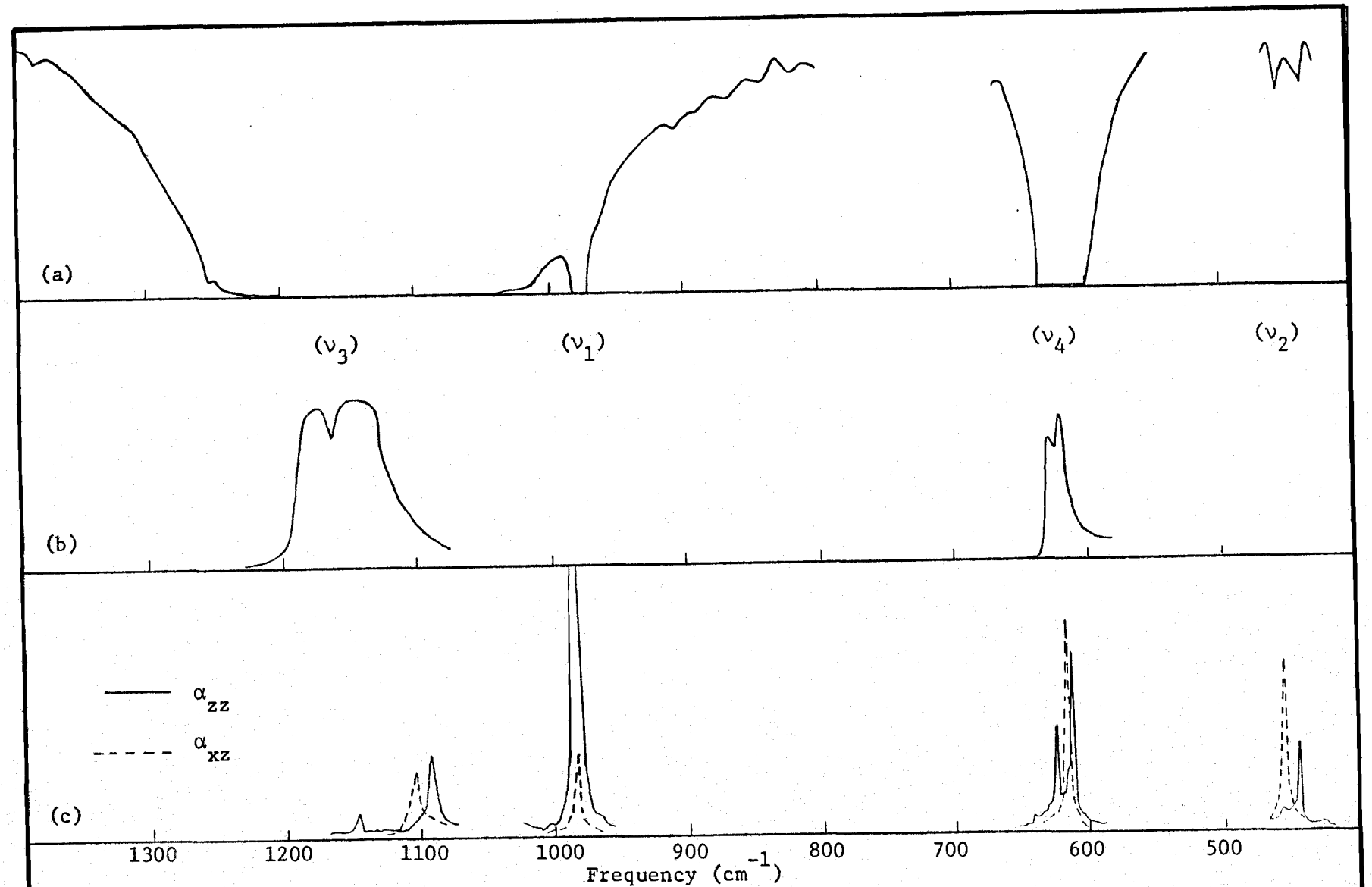

Figure 34. (a) I.R. Transmission, (b) reflection, and (c) Laser Raman spectra of K_2SO_4 under z polarization

Table 10. Experimental Values of the Sulfate Fundamentals in K_2SO_4 Single Crystals

Mode	Frequency	Designation	Source
ν_2	445	A_g	Raman xx,yy,zz
	448	B_{1u},B_{3u}	I.R. Transmission z,y
	452	B_{3g}	Raman yz
	454	B_{2u}	I.R. Transmission y
	455	B_{1g}	Raman xy
	456	B_{2g}	Raman zx
ν_4	613	B_{2u}	I.R. Reflection* y
	615	A_g	Raman xx, yy, zz
	615	B_{3u}	I.R. Reflection* x
	617	B_{1u}	I.R. Reflection* z
	618	B_{3g}	Raman yz
	619	B_{1g},B_{2g}	Raman xy, xz
	622	B_{2u}	I.R. Reflection* y
	624	B_{1u}	I.R. Reflection* z
	627	A_g	Raman xx, yy, zz
ν_1	983	B_{1u},B_{2u}	I.R. Transmission z,y
	984	A_g	Raman xx, yy, zz

Table 10 (Contd.)

Mode	Frequency	Designation	Source
ν_3	1093	A_g	Raman xx, yy, zz
	1104	B_{3u}	I.R. Reflection* x
	1104	B_{1g},B_{2g}	Raman xy, xz
	1108	B_{2u}	I.R. Reflection* y
	1110	B_{3g}	Raman yz
	1121	B_{1u}	I.R. Reflection* z
	1136	B_{2u}	I.R. Reflection* y
	1146	A_g	Raman xx, yy, zz
	1156	B_{1u}	I.R. Reflection* z

* Estimated from low frequency inflections of near-normal reflection spectra.

The utilization of the data pertaining to the resonant vibrational frequencies of the sulfate ion in the K_2SO_4 crystal lattice obtained from infrared transmission and reflection and laser Raman scattering spectra provides a basis upon which an evaluation of the relative effects of site and factor group symmetry can be made. The correlation diagram in Chapter IV shows the correlation of symmetry species of the free ion symmetry, T_d, to the site symmetry, C_s, that the sulfate ion occupies in the lattice and then to the factor group symmetry, D_{2h}^{16}, involving the interionic interactions in the unit cell.

VIII. K_2SO_4 DOPED WITH $(NH_4)_2\ SO_4$

A K_2SO_4 crystal was doped to contain approximately 1% by weight with $(NH_4)_2\ SO_4$. The crystal habit was ascertained by goniometric measurements in order that thin sections could be prepared coplanar with the 010 face. Next, polarized infrared transmission spectra were made and compared to corresponding scans of undoped K_2SO_4 crystals.

A. Growth and Preparation of Crystal

A saturated aqueous K_2SO_4 solution was prepared to which was added 1% by weight $(NH_4)_2\ SO_4$. A small K_2SO_4 seed was suspended in the solution and allowed to grow by solvent evaporation.

When the crystal was large enough, it was harvested and its morphological habit determined. It was found that the long morphological axis corresponded to the unit cell a axis similar to the common habit of undoped K_2SO_4 crystals. A thin section was prepared with faces coplanar with the 010 plane. Using a calibrated microscope to measure the thickness, the crystal was thinned down to 180 ± 5 microns.

The crystal was mounted on a rotatable sample holder which was attached to a beam condenser. A silver chloride multi-plate polarizer was used to polarize the transmitted radiation. The polarizer was kept fixed while the sample was rotated to achieve

the desired alignment of the crystal with the electric vector of the polarized radiation.

Spectra were made with the a axis parallel to the electric vector in one arrangement and with the c axis parallel to the electric vector in the other.

The spectra obtained with the crystalographic a axis of the doped crystal parallel to the electric vector show several features not seen in similar scans of undoped K_2SO_4 (See Figures 11 and 12). A well defined band occurs at 1425 cm^{-1} with a side band at 1460 cm^{-1} and another band is found at 3230 cm^{-1} (See Figures 35 and 36). Spectra obtained when the crystal is rotated 90^o show a band at 1457 cm^{-1} with a weak side band at 1425 cm^{-1} and a band at 3275 cm^{-1}. The structure found near 1400 cm^{-1} corresponds to the NH_4^+ bending mode, ν_4, while that at 3200 cm^{-1} corresponds to the NH_4^+ anti-symmetric stretching mode, ν_3^+. Under T_d symmetry these two modes are both infrared and Raman active and would be triply degenerate. Evidently, the degeneracy is split under the site symmetry of the of the host crystal, K_2SO_4, as opposed to factor group splitting due to coupling of NH_4^+ vibrations. The latter being ruled out due to the apparent diluted state of the ammonium ions in the lattice.

From these preliminary results it seems that the K_2SO_4-$(NH_4)_2SO_4$ system is suited to studying the NH_4^+ under similar surroundings as it experiences in pure $(NH_4)_2SO_4$ crystals. The system allows for

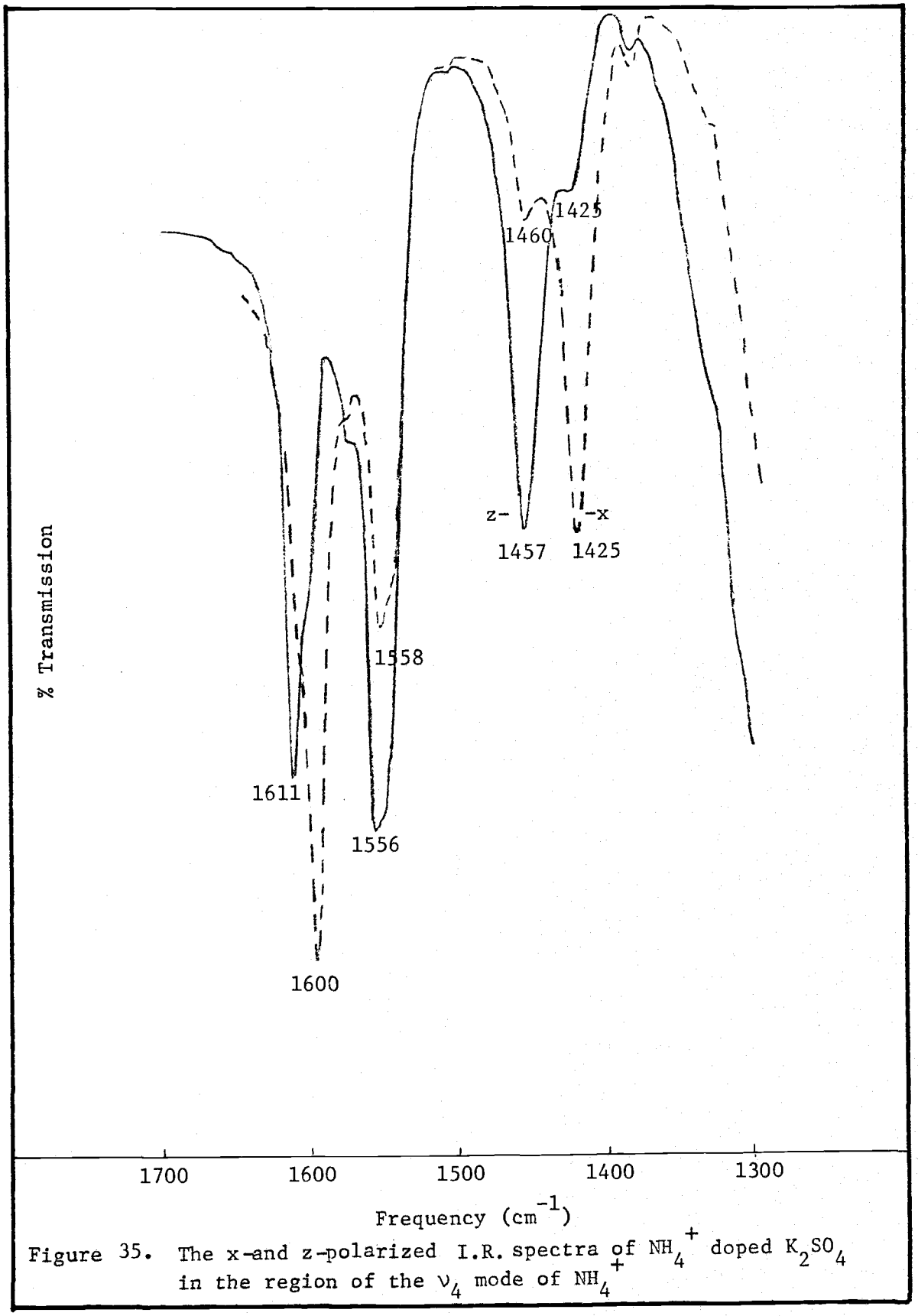

Figure 35. The x-and z-polarized I.R. spectra of NH_4^+ doped K_2SO_4 in the region of the ν_4 mode of NH_4^+

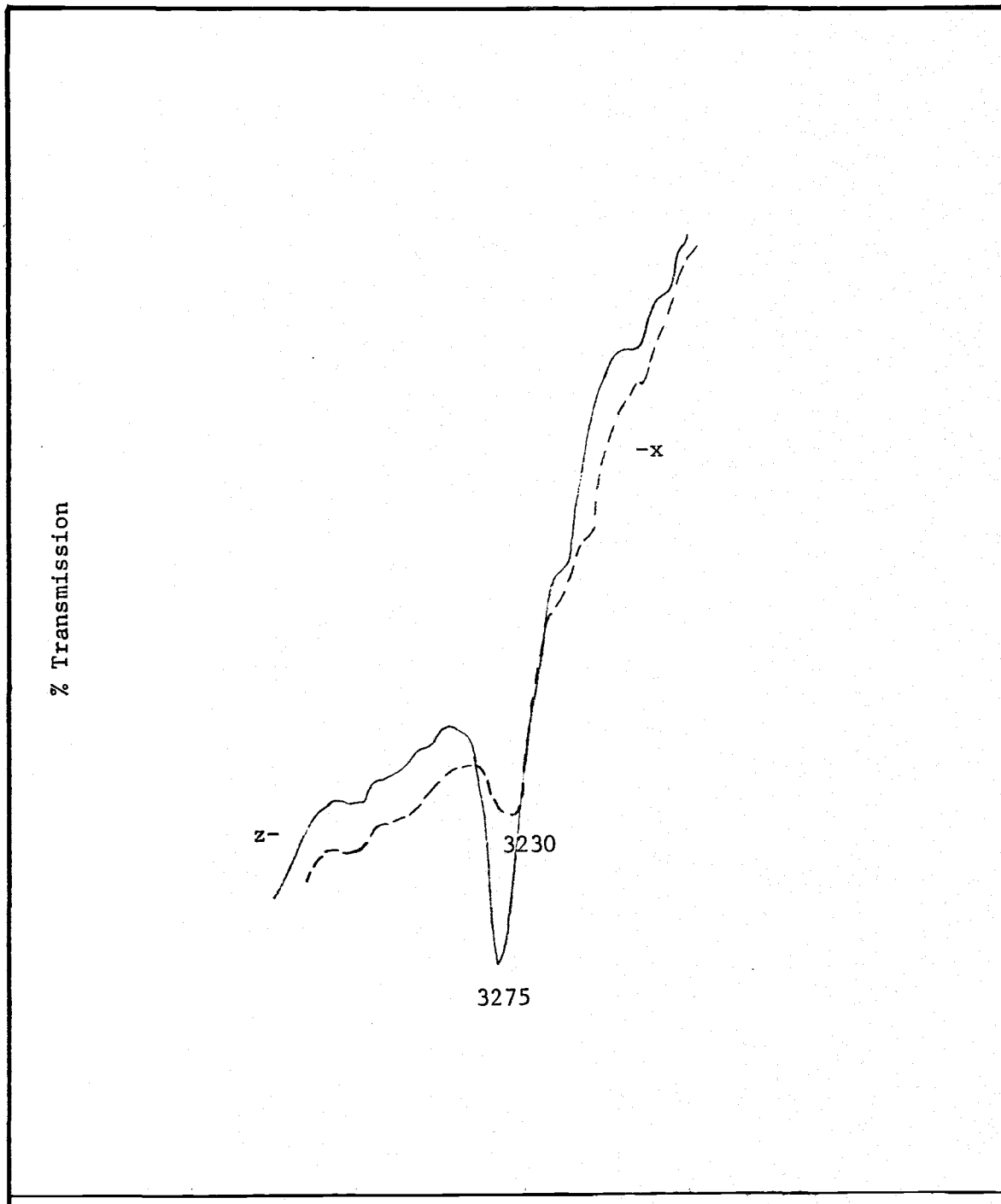

Figure 36. The x-and z-polarized I.R. spectra of NH_4^+ doped K_2SO_4 in the region of the ν_3 mode of NH_4^+

coupling-decoupling measurements by varying the doping ratio. Also the ammonium ion can be studied in the solid state without the severe restriction of obtaining sub-micron single crystaline films.

A thin section of pure $(NH_4)_2SO_4$ was prepared with faces coplanar to the 021 face. The spectrum shown in Figure 37 was obtained from a crystal oriented so as to maximize the small peak at approximately 975 cm^{-1}. The crystal section was less than 20μ thick, however, the crystal was still much too thick to measure the position of the transverse frequency in the three major absorption regions. The band centered at 1100 cm^{-1} is the sulfate vibrational mode, ν_3, with the low frequency side band attributed to sulfate, ν_1. The bands centered at 1430 cm^{-1} and 2890 cm^{-1} are the ammonium vibrational modes, ν_4 and ν_3, respectively.

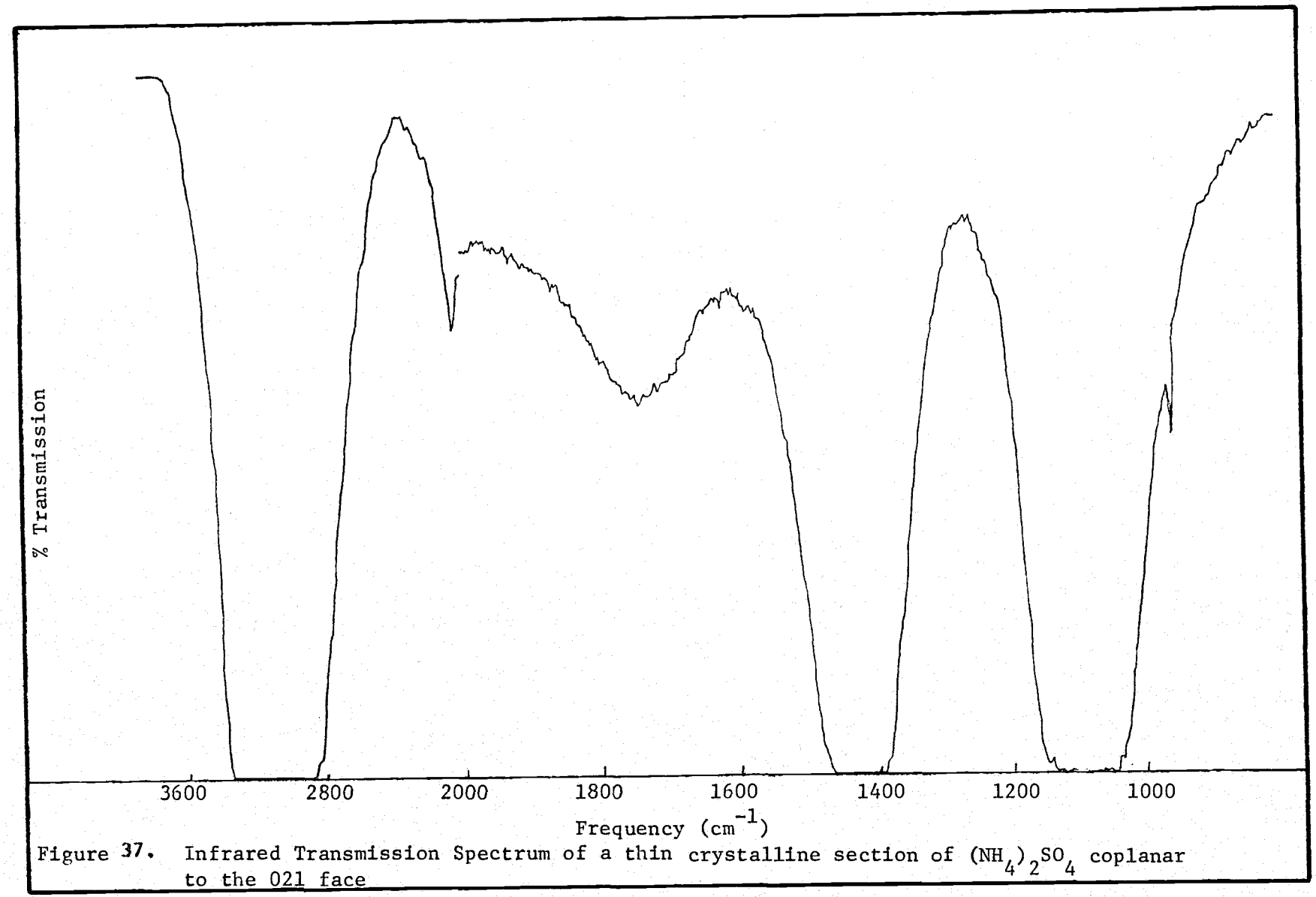

Figure 37. Infrared Transmission Spectrum of a thin crystalline section of $(NH_4)_2SO_4$ coplanar to the 021 face

IX. SUMMARY

The spectral region from 400-4000 cm^{-1} of potassium sulfate was investigated by three optical methods, infrared transmission, infrared reflection and laser Raman scattering. This study of the potassium sulfate crystal system was undertaken to establish its potential as a host matrix for ammonium sulfate.

A reflection goniometer technique was employed to characterize the habit of crystals grown from aqueous solutions. Preparation of additional surfaces parallel to specific planes were monitored for trueness with the goniometer. The combination of selected faces and polarized radiation were used to obtain spectra in which the electric vector was coupled in each of the three principle directions of the molecular vibrations.

The spectra obtained by the three methods are presented in Chapter IV, V and VI, along with a discussion of the major features. The infrared transmission spectra provide little direct information pertaining to the fundamental modes of the sulfate ion. This results from the inability to produce sufficiently thin sections of the potassium sulfate crystals. However, very detailed spectra were obtained in the overtone and combination regions.

The infrared reflection measurements were limited to the sulfate ν_3 and ν_4 modes. Attempts were made to extract information from these spectra to predict the frequencies corresponding to the

maximum absorptions in the limit of very thin films.

The laser Raman spectra give the results of polarized measurements from single crystals of potassium sulfate covering the regions of lattice vibrations and fundamental transitions of the sulfate ion.

Attempts were made throughout to correlate the observed splitting of bands with that predicted from correlation diagrams which invoke both site and factor group splittings. It appears that the splitting due to the low symmetry of the site that the sulfate ion occupies in the lattice is predominant over any intermolecular interactions of the sulfate ions within a unit cell.

Finally, a brief experiment was made to check the feasibility of actually producing ammonium doped potassium sulfate crystals by coprecipitation. The results appear promising as bands attributed to the ammonium ion were observed by infrared transmission measurements.

BIBLIOGRAPHY

1. Ananthanarayanan, V., Indian J. Pure Appl. Phys. 1, 58-60 (1963).

2. Andermann, G. and D. A. Dows, J. Phys. Chem. Solids 28, 1307-1315 (1967).

3. Beaglehole, D., Proc. Phys. Soc. 85, 1007-1020 (1965).

4. Berreman, D. W., Physical Review 130, 2193-2198 (1963).

5. Born, M. and K. Huang, "Dynamical Theory of Crystal Lattices" (Oxford University Press, London, 1954).

6. Born, M. and E. Wolf, "Principles of Optics" (Pergomon Press, Inc., New York, 1965).

7. Buckley, N. E., "Crystal Growth" (Wiley, New York, 1960).

8. Decius, J. C., J. Chem. Phys. 49, 1387-1392 (1968).

9. Decius, J. C., E. H. Coker and G. L. Brenna, Spectochimica Acta 19, 1281-1289 (1963).

10. Decius, J. C., R. Frech and P. Bruesch, "Infrared Reflection from Longitudinal Modes in Anisotropic Crystals" (Manuscript, 1973).

11. Drude, P., "The Theory of Optics" (Dover Publications, Inc., New York, 1959).

12. Frech, R., Post Graduate with J. C. Decius, Oregon State University, Department of Chemistry. Personal communications. Corvallis, Oregon, 1970.

13. Frech, R. and J. C. Decius, J. Chem. Phys. 51, 1536-1541 (1969).

14. Frech, R. and J. C. Decius, J. Chem. Phys. 51, 5315-5322 (1969).

15. Hopfield, J. J., Physical Review 112, 1555-1567 (1958).

16. Hopfield, J. J. and D. G. Thomas, Physical Review 132, 563-572 (1963)

17. Mosteller, L. P. and F. Wooten, J. Opt. Soc. Am. 58: 511-518 (1968)

18. Ogg, A., Phil. Mag. 5, 354-363 (1928)

19. Schroeder, R. A., E. R. Lippincott and C. E. Weir, J. Inorg. Nucl. Chem. 28, 1397-1409 (1966)

20. Wilson, E. B., J. C. Decius and P. C. Cross, "Molecular Vibrations" (McGraw-Hill Book Company, Inc., New York, 1955).

21. Winston, H. and R. S. Halford, J. Chem. Phys. 17, 607-616 (1949).

22. Wyckoff, R. W., "Crystal Structures" (Interscience Publishers, Inc., New York, 1948).